# Cure Kinetics of a Thermosetting Liquid Dicyanate Ester Monomer/High-$T_g$ Polycyanurate Material

S. L. SIMON and J. K. GILLHAM*

Polymer Materials, Department of Chemical Engineering, Princeton University, Princeton, New Jersey 08544

SYNOPSIS

The cure of a liquid dicyanate ester monomer, which reacts to form a high-$T_g$ ($\approx$200°C) polycyanurate network, has been investigated using differential scanning calorimetry (DSC), Fourier transform infrared spectroscopy (FTIR), and a dynamic mechanical technique, torsional braid analysis (TBA). The monomer is cured with and without catalyst. The same one-to-one relationship between fractional conversion and the dimensionless glass transition temperature is found from DSC data for both the uncatalyzed and catalyzed systems, independent of cure temperature, signifying that the same polymeric structure is produced. $T_g$ is the parameter used to monitor the curing reactions since it is uniquely related to conversion, is sensitive, is accurately determined, and is also directly related to the solidification process. The rate of uncatalyzed reaction is found to be much slower than that of the catalyzed reaction. The apparent overall activation energy for the uncatalyzed reaction is found to be greater than that of the catalyzed reaction (22 and 13 kcal/mol, respectively) from time–temperature superposition of experimental isothermal $T_g$ vs. ln time data to form kinetically-controlled master curves for the two systems. Although the time–temperature superposition analysis does not necessitate knowledge of the rate expression, it has limitations, because if the curing process consists of parallel reactions with different activation energies, as is considered to be the case from analysis of the FTIR data, there should not be a kinetically-controlled master curve. Consequently, a kinetic model, which can be satisfactorily extrapolated, is developed from FTIR isothermal cure studies of the uncatalyzed reaction. The FTIR data for the uncatalyzed system at high cure temperatures, where the material is in the liquid or rubbery states throughout cure, 190 to 220°C, are fitted by a model of two parallel reactions, which are second-order and second-order autocatalytic (with activation energies of 11 and 29 kcal/mol), respectively. Using the model parameters determined from the FTIR studies and the relationship between $T_g$ and conversion from DSC studies, $T_g$ vs. time curves are calculated for the uncatalyzed system and found to agree with DSC experimental results for isothermal cure temperatures from 120 to 200°C to even beyond vitrification. The DSC data for the catalyzed system are also described by the same kinetic model after incorporating changes in the pre-exponential frequency factors (due to the higher concentration of catalyst) and after incorporating diffusion-control, which occurs prior to vitrification in the catalyzed system (but well after vitrification in the uncatalyzed system). Time–temperature-transformation (TTT) isothermal cure diagrams for both systems are calculated from the kinetic model and compared to experimental TBA data. Experimental gelation is found to occur at a conversion of approximately 64% in the catalyzed system by comparison of experimental macroscopic gelation at the various curing temperatures and iso-$T_g$ (iso-conversion) curves calculated from the kinetic model. © 1993 John Wiley & Sons, Inc.

## INTRODUCTION

The cure kinetics of a new liquid dicyanate ester monomer, both uncatalyzed and catalyzed, are investigated in this work. The chemical structures of the monomer and polymer are shown in Figure 1. The monomer was commercially introduced in 1990 for use in structural composite, adhesive, coating, and electronic applications,[1] and differs from the more commonly used bisphenol A dicyanate ester monomer in that it is a liquid at room temperature and has a higher molecular weight, which decreases volatility.

* To whom correspondence should be addressed.

Journal of Applied Polymer Science, Vol. 47, 461–485 (1993)
 CCC 0021-8995/93/030461-25

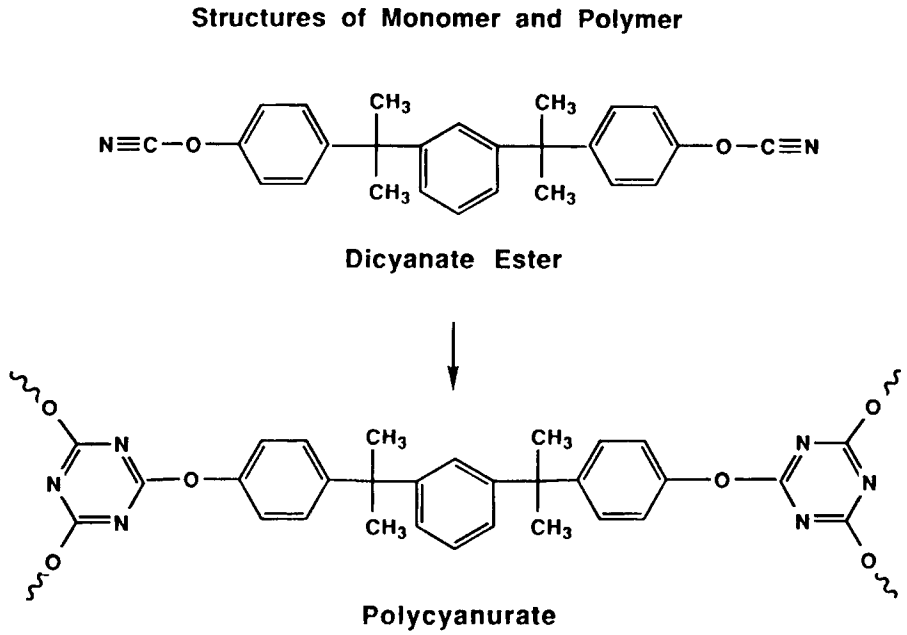


**Figure 1** Structures of monomer and polymer: dicyanate ester reacts to form polycyanurate.

Dicyanate ester monomers generally cure via an addition trimerization reaction, without volatile byproducts, to form high-$T_g$ amorphous thermosetting network materials. The polycyanurate family of polymers displays high $T_g$s, toughness, low moisture absorption, and low dielectric constant and loss.[1,2] The monomer/polymer system has several other properties, which facilitate theoretical study, including high purity and strong characteristic infrared absorption bands for both reactant and product species.

The isothermal time–temperature–transformation (TTT) cure diagram, which was developed for epoxy systems, is a useful intellectual framework for analyzing cure processes of thermosetting systems.[3,4] The TTT diagram, shown in Figure 2, displays the time to reach various events during isothermal cure at different cure temperatures, $T_c$. As a thermosetting material cures, its glass transition temperature, $T_g$, increases from an initial value of $T_{go}$ due to increasing molecular weight, which accompanies a corresponding decrease in the fraction of free volume associated with chain ends (i.e., unreacted cyanate ester groups). Ideal molecular gelation is the incipient formation of infinite molecules that occurs at a specific conversion and at a corresponding $T_g$ of ${}_{gel}T_g$. For the dicyanate ester/polycyanurate system studied in this work, ideal molecular gelation will theoretically occur at a conversion of 50%[5]; in contrast, macroscopic gelation, which can be associated with an isoviscous state, occurs at an experimental conversion of approximately 64% (see below). After molecular gelation, $T_g$ increases due to increasing crosslink density, as well as to increasing number average molecular weight (of the sol/gel mixture) and decreasing number of chain ends. As $T_g$ approaches the temperature of cure, the material enters the glass transition region and is defined to vitrify or solidify when $T_g$ equals $T_c$. In an ideal system, gelation and vitrification would occur simultaneously at a cure temperature ${}_{gel}T_g$. The reaction may become progressively diffusion-controlled as the segmental mobility decreases during cure. In this work, diffusion control is found to be insignificant in the uncatalyzed system to beyond vitrification for the timescales investigated, whereas it occurs in the rubbery state prior to vitrification in the catalyzed system. In contrast, for a high-$T_g$ epoxy/amine system, the onset of diffusion control was associated with vitrification.[6–8] After vitrification, the reaction rate is affected by both chemical reaction and physical aging: the segmental mobility decreases with increasing chemical conversion corresponding to an increase in $T_g$; and the segmental mobility decreases with time due to physical aging, which occurs when a material is in the nonequilibrium state below its glass transition. If the cure temperature is above the $T_g$ of the fully cured material, $T_{g\infty}$, the material cannot vitrify at $T_c$.

A kinetic mechanism for the aryl phenol/triazine

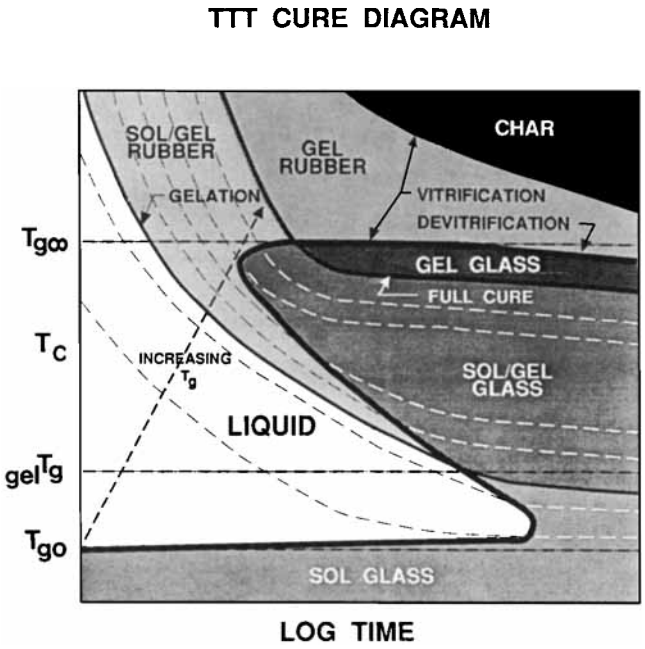


**Figure 2** Generalized time–temperature–transformation (TTT) isothermal cure diagram. From *J. Appl. Polym. Sci.*, **41**, 2885–2929 (1990).

catalyzed trimerization reaction of dicyanate esters has been proposed.[9] The researchers observed that, although dicyanate esters can be homopolymerized, no reaction will take place if absolutely pure aromatic dicyanate ester is heated. Their proposed mechanism for the reaction of an aromatic dicyanate ester involves cyanate ester reacting with aryl phenol impurity under triazine catalysis to produce an imidocarbonate intermediate, which then reacts with two cyanate groups to form triazine and to regenerate the aryl phenol. Their proposed start-up reaction in the absence of the triazine product involves catalysis by adventitious water and aryl phenol, both of which are assumed to be present in the monomer. Calculations, based on the proposed model, fitted the experimental data to approximately 60% conversion. Activation energies of 53 and 84 kJ/mol (13 and 20 kcal/mol) were found for the reaction to form imidocarbonate and the reaction of imidocarbonate to triazine, respectively. The researchers separately described the overall reaction, again to approximately 60% conversion, by first order kinetics with an overall activation energy of 80 kJ/mol (20 kcal/mol).[9]

The mechanism for the water/chromium acetylacetonate catalyzed trimerization of a dicyanate ester has been investigated by other researchers.[10] Their model involves reaction of the monomer with catalyst to form a metal complex intermediate with reduced electron density at the carbon of the cyanate group, which then reacts stepwise with the nucleophilic nitrogens of other cyanate groups to form the triazine and regenerate the metal complex intermediate.

Concurrently with the research presented in this work, another group of researchers has modeled the uncatalyzed and catalyzed reactions of bisphenol A dicyanate and has examined the effects of various catalysts.[11-13] Their model for catalyzed systems, which is second-order with respect to cyanate concentration and first-order with respect to metal catalyst concentration, fits their experimental FTIR conversion vs time data to beyond gelation for cure temperatures from 130 to 200°C,[12-13] but appears to deviate from the data in the rubbery state when $T_g$ is approximately 50 to 70°C below $T_c$. The model for the uncatalyzed system consists of two additive terms, which are first-order plus first-order autocatalytic with respect to cyanate concentration.[12] Diffusion-control is not incorporated into either of the models. In contrast, in the present work, one model consisting of two terms, with diffusion-control incorporated, is invoked to describe both the uncatalyzed and catalyzed systems studied.

The particular dicyanate ester monomer studied in the present work was chosen on the basis of preliminary experiments on several other then-available dicyanate ester systems.[8] The cure of both uncatalyzed and catalyzed systems are studied using differential scanning calorimetry (DSC), Fourier

transform infrared spectroscopy (FTIR), and a dynamic mechanical technique, torsional braid analysis (TBA). The glass transition temperature, $T_g$, which is found to be related to fractional conversion in a one-to-one manner, is used as a direct measure of conversion in the DSC work, rather than using the conversion obtained by the residual heat of the reaction, because $T_g$ is more sensitive and more accurately measured.[6] The relationship between $T_g$ and conversion is further investigated. A mathematical model of the cure kinetics of the uncatalyzed system is determined from FTIR studies in a limited and high temperature range, and is then checked for consistency by comparing calculated and experimental DSC data in a wider temperature range. The model is also applied to the catalyzed system with the incorporation of diffusion control. Time–temperature–transformation (TTT) isothermal cure diagrams are calculated for both systems from the kinetic model and compared to isothermal TBA data.

Preliminary work in this laboratory on the cure and physical aging of the subject dicyanate ester/polycyanurate system has been published.[14-16] "Anomalous" behavior of properties in the glassy state (e.g., the modulus at a fixed temperature passes through a maximum with increasing extent of cure) has also been investigated.[8,17-19] A more complete report is available.[8]

## MATERIALS

The thermosetting system investigated is a liquid dicyanate ester, derived from 4,4′-[1,3-phenylene bis(1-methylethylidene)] bisphenol, (Rhône–Poulenc High Performance Resins, RTX366) cured without catalyst and with catalyst. A $^{13}C$ NMR spectrum of the uncatalyzed monomer, shown in Figure 3, demonstrates the purity and confirms the chemical structure of the monomer.[20] In the $^{13}C$ NMR spectrum, the two aliphatic carbons are associated with the upfield peaks, whereas the downfield peaks are associated with the eight aromatic carbons. The unsplit peak associated with the cyanate carbon is at approximately 107 ppm.[21] A proton NMR spectrum[20] is shown elsewhere.[8]

The catalyzed system consists of 100 parts by weight monomer and 2 parts by weight of added catalyst. The added catalyst is 8.5 wt % copper naphthenate (8 wt % of which is copper) in 91.5 wt % nonylphenol (Rhône–Poulenc High Performance Resins, ESR 273). The added metal ion concentration in the catalyzed system corresponds to 136 ppm

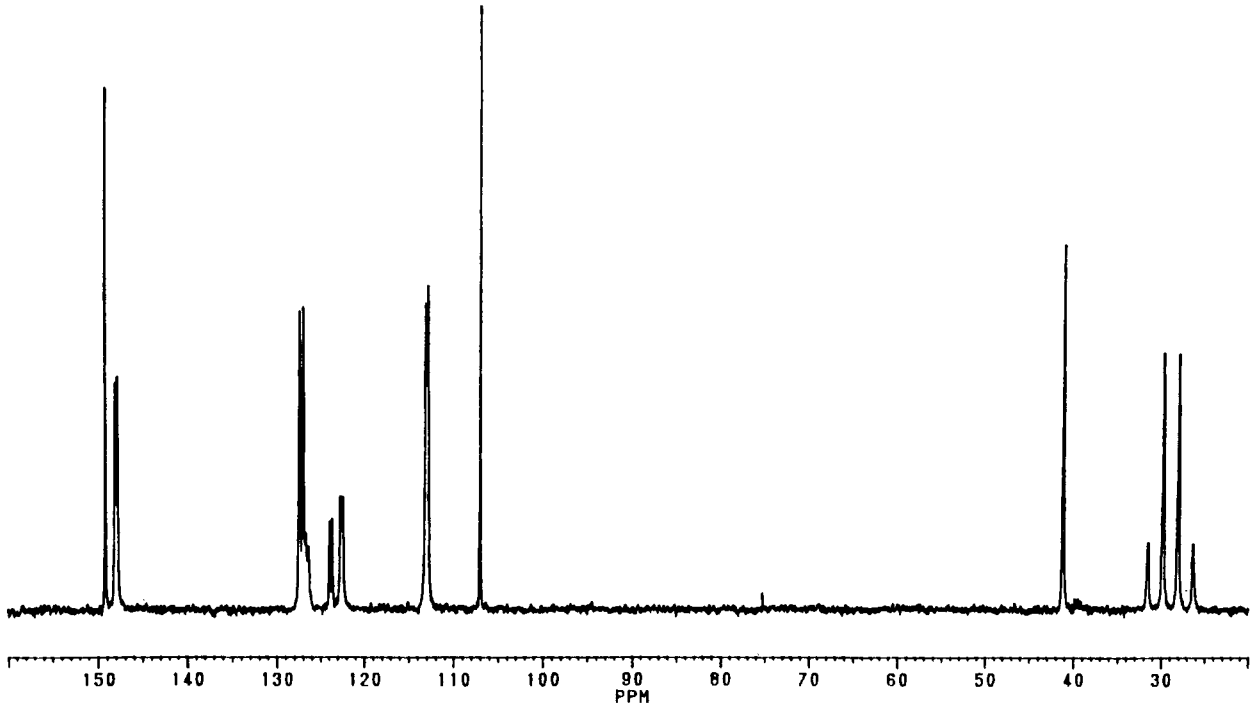


**Figure 3** $^{13}C$ NMR spectrum of uncatalyzed monomer, with dimethyl sulfoxide –d6 as the external reference, acquired under weak decoupling in the melt at 60°C.[20]

by weight per total weight, whereas the added nonylphenol concentration corresponds to 1.7 mol % per mole of cyanate groups. Before adding the catalyst, the monomer is heated to 100°C for 3 min to remove any crystallites formed during prolonged storage in the freezer ($\approx -15$°C) and then is allowed to cool to room temperature. The catalyst is added dropwise during mechanical stirring. Both the catalyzed and uncatalyzed samples are stored in a dessicator in the freezer until needed. No crystallites formed in the catalyzed system during cold storage. No attempt was made to exclude air during mixing or storage.

The glass transition temperature of the amorphous monomer without catalyst is −26°C by DSC at 10°C/min and −15°C by TBA at 1°C/min (from the maximum in logarithmic decrement). The melting temperature of the monomer is 41°C by DSC. The maximum experimental value of $T_g$ for the "fully-cured" polymeric network, $T_{g\infty}$, is approximately 198 and 204°C by DSC and TBA, respectively, for the uncatalyzed system. $T_{g\infty}$ for the catalyzed system, in which the nonylphenyl catalyst acts as a plasticizer, is lower at 182 and 190°C, respectively. The monomer was specifically synthesized for the project by W. M. Craig of Rhône–Poulenc High Performance Resins on the basis of our need for a pure, non-volatile liquid monomer for scientific investigations, since preliminary work on other lower molecular weight dicyanate ester monomers was complicated by volatility.[8]

## EXPERIMENTAL PROCEDURES

A Perkin–Elmer DSC-4 unit was used for differential scanning calorimetry. Five to ten milligrams of the uncured monomer, either uncatalyzed or catalyzed, were sealed in aluminum pans and cured in the DSC itself under nitrogen purge at cure temperatures, $T_c$, from 100 to 200°C and for cure times ranging from 1 to 24 h. Samples cured from 24 h to 4 weeks were cured in a nitrogen-purged press oven, rather than in the DSC. The DSC-cured samples were cooled to −30°C at 10°C/min, whereas the oven-cured samples were free-cooled to room-temperature and placed in the DSC and cooled to −30°C at 10°C/min. The samples are then scanned from −30 to 380°C at 10°C/min. No discrepancy between the two curing methods was observed. Samples, which have vitrified during cure ($T_g > T_c$), show an endothermic physical aging peak in the vicinity of $T_g$.[8] In order to eliminate the physical aging peak and, therefore, the effects of physical aging on $T_g$, the sample was quenched to −30 at 320°C/min after scanning up to just beyond the aging peak, and then rescanned from −30 to 380°C at 10°C/min. This procedure has been described in other work from our laboratory[6,8] and does not affect the measured value of $T_g$ significantly: calculations based on the proposed kinetic model of the reaction (see below) demonstrate that the increase in $T_g$ is less than 0.1°C for the uncatalyzed system and less than 0.5°C for the catalyzed system, both within the error of the measurement of approximately ±1°C.[8]

The DSC scans yield the glass transition, $T_g$, and the exothermic residual heat of reaction. The total heats of reaction are −100 and −96 kJ/mol of cyanate groups (−24 and −23 kcal/mol), for the uncatalyzed and catalyzed systems, respectively. The error in the total heats is considered to be approximately 5%. The similarity of the heats of reaction for the two systems indicates that the same reactions occur in the two systems. The heats compare favorably to those found in preliminary studies of 4,4′-dicyanato 2,2-diphenylpropane, commonly referred to as bisphenol A dicyanate, and 4,4′-dicyanato 1,1-diphenylethane (Arocy B10 and Arocy L10, Rhône–Poulenc High Performance Resins, respectively), which displayed heats of −89 and −110 kJ/mol of cyanate for the uncatalyzed systems, respectively, and −87 and −90 kJ/mol of cyanate for the catalyzed systems, respectively.[8] Other researchers report values of the heat of bisphenol A dicyanate polymerization of −104 kJ/mol of cyanate (20°C/min),[22] −105 kJ/mol (10°C/min),[10] and −110 kJ/mol (10°C/min),[9,23] whereas yet another group of researchers report that the heat is −97 ± 14 kJ/mol of cyanate (20°C/min) and attribute the error band to volatility of the monomer.[24] Researchers associated with the synthesis of the dicyanate ester studied in this work report that the heat of polymerization for various dicyanate ester monomers ranges from −92 to −100 kJ/mol of cyanate.[2]

The DSC conversion is determined for a partially cured sample by:

$$x(\mathrm{DSC}) = \frac{(\Delta H_T - \Delta H_r)}{\Delta H_T} \qquad (1)$$

where $\Delta H_T$ is the total heat of reaction of an initially uncured sample and $\Delta H_r$ is the residual heat for a partially cured sample.

Infrared spectroscopy is accomplished using a Nicolet 170SX spectrometer with a mercury cadmium telluride (MCT) detector. A closed, nitrogen-purged, Harrick heating cell is used to cure uncatalyzed samples *in situ* at five cure temperatures from 190 to 220°C (i.e., in the liquid or rubbery

states, since at lower cure temperatures vitrification can affect the infrared absorption coefficients). NaCl salt plates are polished, heated to above 100°C, and then placed in the nitrogen-purged FTIR bench to minimize absorbed moisture prior to placing the liquid monomer between them. Care is taken in sample preparation in order to prevent trapping air bubbles in the sandwiched sample, which can cause spurious absorption peaks in the vicinity of gelation (and vitrification). The sample is then placed in the heating cell, which is maintained at 100°C, and the cell is placed in the FTIR apparatus. The system is purged with nitrogen for 30 min, during which the sample does not react due to the low rate of reaction of the uncatalyzed system (the fractional conversion is less than 0.001 after 30 min at 100°C, based on the kinetic model, see below). An IR scan is taken to check for water. The temperature is then ramped up to the curing temperature at 10°C/min. The sample is cured for approximately one day at the temperature of cure, with approximately 88 spectra obtained at increasing time intervals.

Torsional braid analysis (TBA) is a dynamic mechanical technique in which a monomer-impregnated fiberglass braid specimen is part of a freely oscillating torsion pendulum.[25] The pendulum is intermittently torqued through a small angle and allowed to oscillate at its resonance frequency ($\approx$1 Hz). The period and damping of the oscillations yield mechanical parameters of the specimen, namely relative rigidity, which is proportional to the shear modulus ($G'$) and the logarithmic decrement, which is proportional to $G''/G'$, where $G''$ is the shear loss modulus. Isothermal cure studies at temperatures from 80 to 210°C for times up to 1 month were accomplished under slow flowing helium gas. From the peaks in the logarithmic decrement, the times to macroscopic gelation, considered to be an iso-viscous event, and the times to vitrification, which occurs when $T_g$ rises to the cure temperature, are determined for the various cure temperatures. An experimental time–temperature–transformation (TTT) isothermal cure diagram, which displays the times to gelation and vitrification at different isothermal curing temperatures, is constructed from the data. The automated TBA torsion pendulum system is available from Plastics Analysis Instruments, Inc., Princeton, NJ.

## RESULTS AND DISCUSSION

### DSC Studies: $T_g$ vs. Conversion Relationship

Preliminary DSC results have been published for the dicyanate ester/polycyanurate system studied, which showed a one-to-one relationship between $T_g$ and fractional conversion, $x$, independent of cure temperature.[14] Similar results are found for other dicyanate ester systems[8,11,26] and for high-$T_g$ epoxy/amine systems.[6,7,27,28] Consequently, $T_g$ can be used as a measure of conversion. This is of practical importance because $T_g$ is more easily and accurately measured than conversion, especially at high conversions where $T_g$ is increasing but there is little or no measurable change in the residual heat from DSC scans. Thus, it is appropriate to use the $T_g$ as the primary variable and to transform $T_g$ to conversion and vice versa, when necessary, via the one-to-one relationship obtained from a theoretical or empirical fit of the experimental data. For example, to test a kinetic model, the conversion is calculated as a function of time and cure temperature from the model equations, transformed to $T_g$ and then compared to experimental $T_g$ data. Note that any physical aging that occurs during cure (e.g., if the material vitrified during cure) should be erased prior to measuring $T_g$ by DSC, as described in the experimental procedure, in order to obtain the one-to-one relationship between $T_g$ and conversion.

It is considered that the one-to-one relationship occurs when the chemical structure is not dependent on cure path, that is, when there is only one product formed by the curing reaction(s), as in this and other dicyanate ester systems,[2,29] or when competing reactions yielding different structures have similar activation energies or occur sequentially, as in a high-$T_g$ epoxy/amine system studied in this laboratory.[7,8] The relationship may also be observed even when competing reactions with unequal activation energies yield different networks. For example, although the concentration of dangling chain ends, branch points, and polarity are dependent on the ratio of the rate constants of the competing reactions of epoxy with primary and with secondary amines in a high $T_g$ epoxy/amine system, it has been shown that the crosslink density and number-average molecular weight, and hence $T_g$, assuming that $T_g$ is a function of these two parameters, are insensitive to the ratio of the competing reactions.[28] It is also noted that $T_g$ is an average network property over a certain unknown length scale so that some of the specific characteristics of a network may not be of importance. In other words, $T_g$ may not be sensitive to some details of the specific molecular structure. Consequently, a one-to-one relationship between $T_g$ and conversion independent of cure temperature, for the case of competing reactions with different activation energies, will depend on the sensitivity of $T_g$ to the various network parameters, which in turn may or may not be sensitive to the ratio of the rates of the competing reactions.

The experimental $T_g$ vs. conversion DSC data are shown in Figures 4 and 5 for the uncatalyzed and catalyzed systems, respectively. The data for the uncatalyzed system show considerably more scatter than does the catalyzed system due to the volatility of the material, which is inherently low but becomes significant due to the long curing times of the uncatalyzed material (the time to vitrify at 150°C is approximately four days). The effects of adventitious water when DSC sample pans are sealed in air, rather than under nitrogen, also produces scatter in the results for the uncatalyzed system. (In retrospect, all of the samples should have been sealed under nitrogen.) Due to the much faster cure of the catalyzed system, volatility and the effects of adventitious water are less significant, and the $T_g$ vs conversion data show correspondingly less scatter. Since the uncatalyzed and catalyzed systems both are presumed to have the same network structure with the main difference being that the catalyst will plasticize the catalyzed material and lower its $T_g$, it is of interest to appropriately scale $T_g$, as follows, so that a more accurate $T_g$ vs conversion relationship for the uncatalyzed system can be obtained.

The empirical DiBenedetto equation[30] has recently been rewritten in a modified form derived from entropic considerations of an idealized simple system consisting of a mixture of fully-cured network and monomer:

$$\frac{T_g - T_{go}}{T_{g\infty} - T_{go}} = \frac{\lambda x}{1 - (1 - \lambda)x} \tag{2}$$

where $T_{go}$ is the $T_g$ of the uncured monomer, $T_{g\infty}$ is the maximum $T_g$ obtained experimentally for the "fully-cured" material, and $\lambda$ is taken as a structure-dependent parameter.[31] The plot of $(T_g - T_{go})/(T_{g\infty} - T_{go})$ vs. $x$ for both the uncatalyzed and catalyzed systems, Figure 6, shows that the above equation is, indeed, an appropriate scaling of the data since one master curve is obtained. The parameter $\lambda$ is theoretically equated to $\Delta C_{p\infty}/\Delta C_{po}$, where $\Delta C_{p\infty}$ and $\Delta C_{po}$ are the differences in heat capacity between the glassy and rubbery (or liquid, prior to gelation) states at $T_g$ for the fully-cured network and monomer, respectively.[31] Due to the scatter in the experimental values of $\Delta C_p$, $\lambda$ is treated as an adjustable parameter and is determined to be 0.426 from a plot of $(T_{g\infty} - T_{go})/(T_g - T_{go})$ vs. $1/x$.[8] Comparatively, the experimental value of $\Delta C_{p\infty}/\Delta C_{po}$ is approxi-

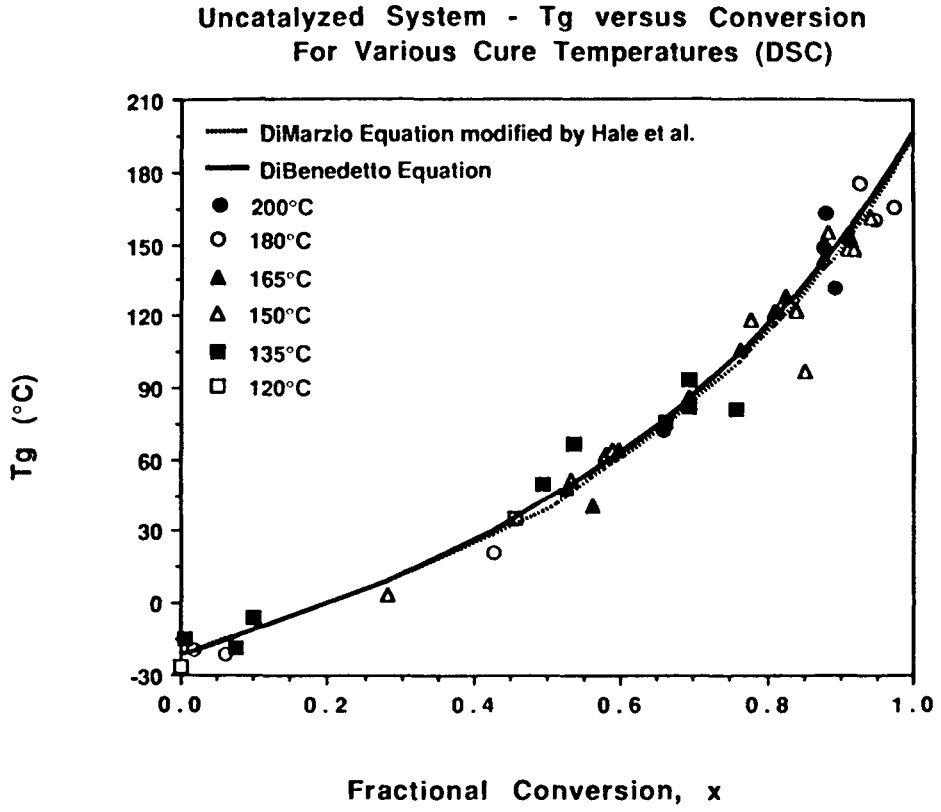


**Figure 4** One-to-one relationship between $T_g$ and conversion, independent of cure temperature, for the uncatalyzed system.

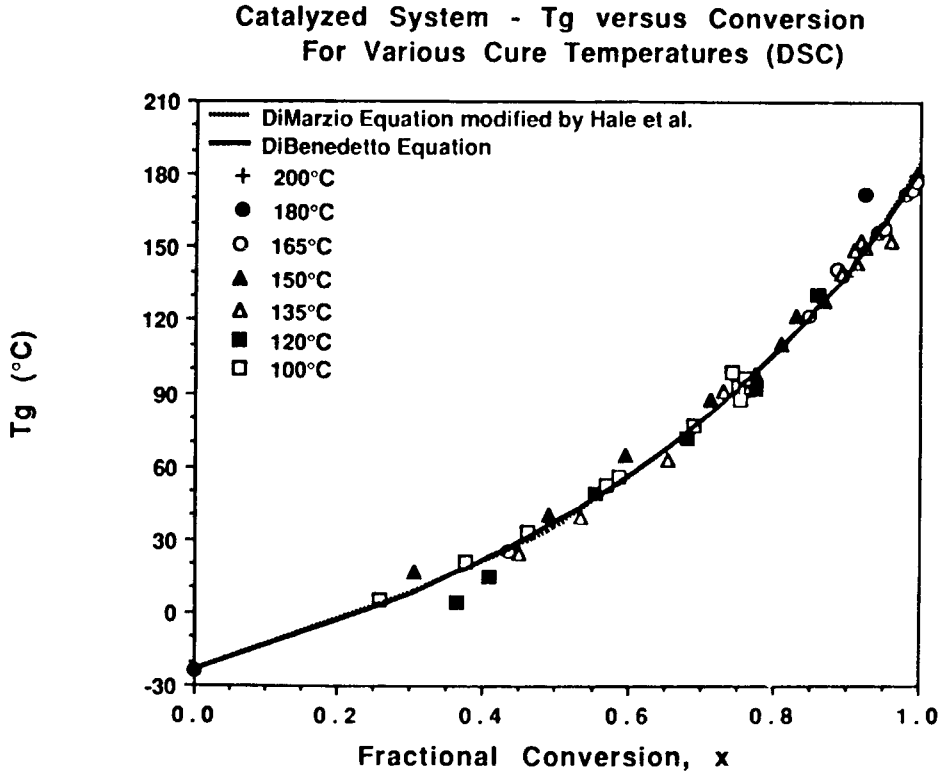


**Figure 5** One-to-one relationship between $T_g$ and conversion, independent of cure temperature, for the catalyzed system.

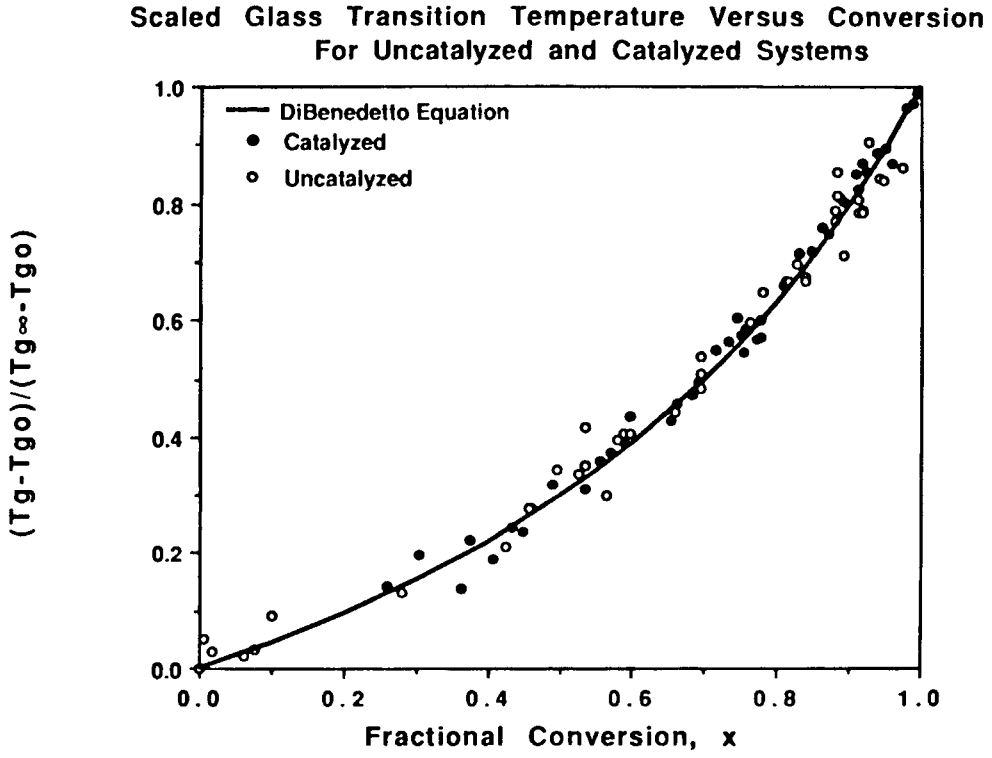


**Figure 6** Dimensionless glass transition temperature vs. conversion for the uncatalyzed and catalyzed material showing the one-to-one relationship for all data.

mately 0.6 ± 0.1 for both uncatalyzed and catalyzed systems.

It is noted that eq. (2) is a one parameter model, with the value of λ dictating the curvature of the $T_g$ vs. conversion relationship.[31] For systems with different structures, the parameter λ will change. From limited data of two other dicyanate ester systems, bisphenol A dicyanate and 4,4′-dicyanato 1,1-diphenylethane, λ is estimated to be 0.3 and 0.4, respectively.[8] Other researchers have found λ to be 0.27 for 4,4′-dicyanato 1,1-diphenylethane.[26] It is not expected that the DiBenedetto equation will model complicated $T_g$ vs. conversion relationships, as in an epoxy-rich epoxy/amine system studied in other work from this laboratory, where sequential reactions produce different types of crosslinks.[7,8] A different equation,[32] which is based on network parameters, was used in order to fit data for two off-stoichiometric epoxy/amine systems with the same network parameters. Although not necessary in the present work, this alternative equation is tested here for its application to the dicyanate ester/polycyanurate system studied.

The recently published equation[32] separately accounts for the effects of chain ends and branching, crosslink density, and the non-Gaussian nature of crosslinks at high conversions on $T_g$:

$$T_g(x) = T_{gu}(x)\left(\frac{1}{1 - \dfrac{KX}{1 - \Psi X^2}}\right) = \left(\frac{1}{\dfrac{1}{T_{go}} - kx}\right)\left(\frac{1}{1 - \dfrac{KX}{1 - \Psi X^2}}\right) \quad (3)$$

where $T_{gu}(x)$ is the glass transition temperature of the uncrosslinked system at a conversion $x$ (hypothetical after gelation), $T_{go}$ is the initial glass transition temperature of the unreacted material, and $X$ is the crosslink density. In this work, a branch point is a triazine ring and a crosslink point is a branch point whose three arms are part of the infinite gel network.

The constant $k$ is considered in this work to be proportional to the concentration of chain ends, $C_o(1 - x)$, where $C_o$ is the initial concentration of cyanate in moles cyanate groups per total moles cyanate groups and catalyst.[8] Since $C_o$ is approximately the same for both uncatalyzed and catalyzed systems (the catalyst is only 2 wt % and 3 mol % of the catalyzed system), $k$ is considered to be the same constant for both systems. The effect of branching is implicitly incorporated into eq. (3), since the concentration of branch points and chain ends are inversely related: every branch point results in the loss of three ends.

The constant $K$ in eq. (3) incorporates the effects of crosslinks on the glass transition temperature. $K$ was originally considered to be a universal constant, but has been shown to vary with monomer structure.[32] The constant $\Psi$ incorporates the effects of non-Gaussian behavior of segments at high crosslink density (as observed by behavior in the rubbery state), and should vary with segment length, stiffness, and polarity. Since it is presumed that the network structures of the uncatalyzed and catalyzed systems are the same, both $K$ and $\Psi$ are considered to be the same constant for the two systems.

The crosslink density is calculated using the recursive method of Miller and Macosko.[33] Following the notation of Miller and Macosko, the crosslink density, $X$, is:

$$X = \frac{C_o}{3}[1 - P(F_C^{\text{out}})]^3 \quad (4)$$

where $P(F_C^{\text{out}})$ is the probability of finding a finite chain looking out from a cyanate group. The probability of finding a finite chain is determined assuming that only the cyanate trimerization reaction occurs, that no intramolecular reactions occur in finite species (i.e., only the treelike structure exists in the finite species), that the reactivity is independent of molecular size, and that the reaction is homogeneous. The probability of finding a finite chain lies between 0 (corresponding to full conversion where $x = 1$) and 1 (prior to ideal molecular gelation, which occurs at $x = 0.5$). The probability of finding a finite chain looking out from a cyanate group is found by solving the following equations for the probability of finding a finite chain looking out from, $P(F_C^{\text{out}})$, and looking in towards, $P(F_C^{\text{in}})$, a cyanate group:

$$P(F_C^{\text{out}}) = xP(F_C^{\text{in}})^2 + 1 - x \quad (5)$$

$$P(F_C^{\text{in}}) = P(F_C^{\text{out}}) \quad (6)$$

Thus,

$$P(F_C^{\text{out}}) = P(F_C^{\text{in}}) = \frac{1 - \sqrt{1 - 4x(1 - x)}}{2x} \quad (7)$$

The parameter $k$ is determined from a plot of $1/T_{go} - 1/T_g$ vs. $x$, using data from both systems prior to gelation ($x \leq 0.5$, $X = 0$), to be 0.0015.[8] The parameters $K$ and $\Psi$ are determined to be 0.13

and 6.0 from a plot of $\frac{X}{\left(1-\left(\frac{1}{T_g}\right)\Big/\left(\frac{1}{T_{go}}-kx\right)\right)}$ versus $X^2$, again combining data for both systems.[8]

The $T_g$ vs. conversion curves from eq. (3), plotted in Figures 4 and 5 as dashed lines, are nearly indistinguishable from the solid curves derived from the DiBenedetto equation. Either relation could be used to describe the experimental data, in contrast with the series of off-stoichiometric epoxy/amine systems, in which only eq. (3) can be used.[7,8] In this work, due to its simplicity, the DiBenedetto equation will be used when it is necessary to convert $T_g$ to conversion and vice versa.

## Time–Temperature Superposition of DSC Data

$T_g$ increases with time of reaction from $T_{go}$, as shown in Figures 7 and 8 for the uncatalyzed and catalyzed systems, respectively. At the highest cure temperatures, $T_g$ levels off at the maximum observed $T_g$ of the network, $T_{g\infty}$, and then decreases for the catalyzed system at the highest cure temperatures, presumably due to degradation reactions. The scatter in the experimental data for the uncatalyzed system is presumed to be due to the presence of adventitious water from air in the sealed DSC sample pans. Assuming that the curing reactions can be described by an overall Arrhenius rate expression with only one activation energy (i.e., one reaction, or several reactions having the same activation energy), a kinetically-controlled master curve of the curing reactions can be obtained by time–temperature superposition of the $T_g$ vs. ln time data at an arbitrary reference temperature. The basis for such a shift is the one-to-one relationship between $T_g$ and conversion, the assumption that the reaction is kinetically controlled in the shifted regime, and the assumption that the reaction(s) can be described by one activation energy.[6,34]

Figures 9 and 10 show the attempts to obtain kinetically-controlled master curves for the uncatalyzed and catalyzed systems, respectively. The onset of diffusion-control is readily apparent in the catalyzed system, with data branching off from the master curve. This deviation of data from the master curve is considered not to be due to a change in the reaction or reaction mechanism, since the deviation

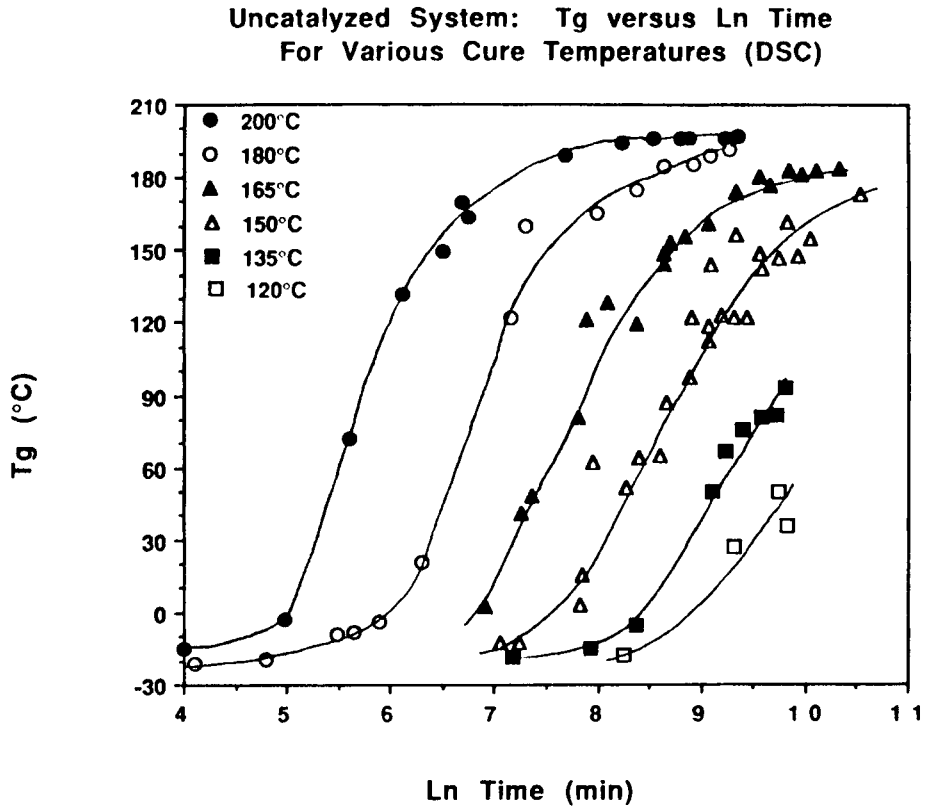


**Figure 7** $T_g$ vs. Ln time for various cure temperatures for the uncatalyzed system from DSC isothermal cure studies. Symbols are the experimental data; full lines are hand-fit.

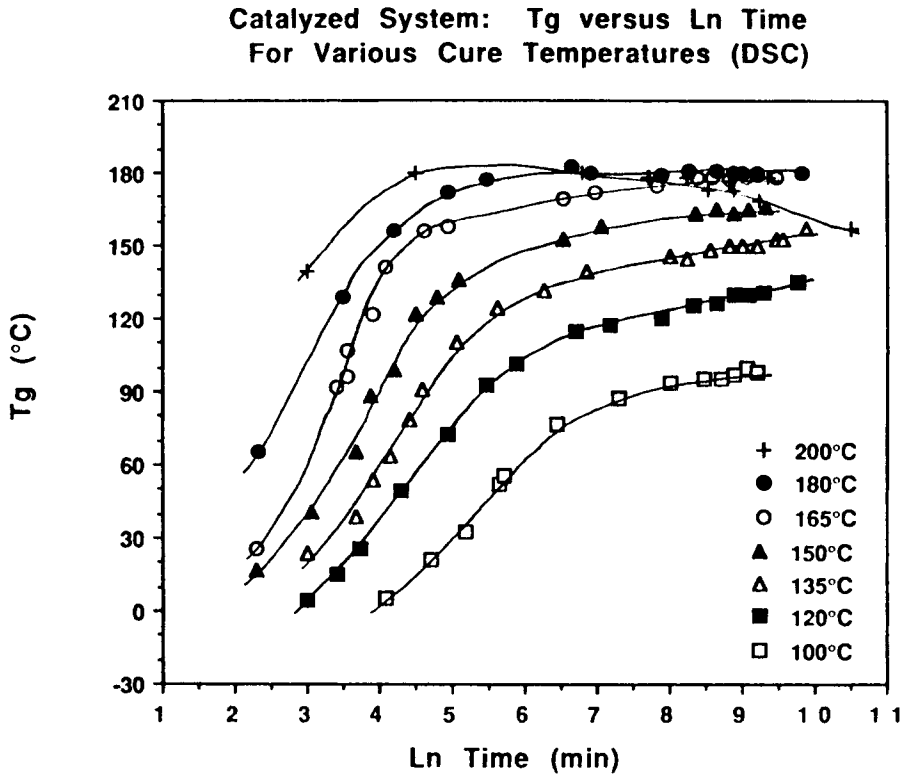


**Figure 8** $T_g$ vs. Ln time for various cure temperatures for the catalyzed system from DSC isothermal cure studies. Symbols are the experimental data; full lines are hand-fit.

occurs at different conversions ($T_g$s) for the different cure temperatures (in contrast to the change in reaction observed after amine depletion at a particular conversion in an epoxy-rich system studied in this laboratory[7,8]). The onset of diffusion-control in the catalyzed dicyanate ester system occurs in the rubbery state prior to vitrification (designated by arrows in Figure 10), in contrast to the behavior in a high-$T_g$ epoxy/amine system studied in this laboratory, in which the onset of diffusion control occured slightly after vitrification.[6-8] In the uncatalyzed dicyanate ester system, there is some evidence of deviation from the master curve at high conversions. However, this is shown later in this work to be the result of both diffusion control and the competition between two reaction paths with different activation energies, which complicate the time–temperature superposition procedure. Consequently, the results of time–temperature superposition should be viewed with reservation until it is shown that all of the reactions needed to describe the curing process have the same activation energy. Nevertheless, for use in a limited temperature range, the time–temperature superposition is a useful tool for investigating the overall temperature dependence of the curing reactions.

In the trimerization reaction, the onset of diffusion control might be expected to occur earlier than in curing reactions involving only two reacting groups, as in the epoxy/amine reaction, due to an increase in the time of diffusion for the three groups to come together. However, the timescale of the chemical reaction in the absence of diffusion is also a factor, since the onset of diffusion control occurs when the timescales of diffusion and of the chemical reaction are of the same magnitude. During isothermal cure, the timescale of chemical reaction, the reciprocal normalized rate constant ($\text{time}^{-1}$), is constant (neglecting the effect of volume changes, which occur during cure), whereas the timescale of diffusion increases as segmental mobility and the concentration of reacting groups both decrease. The diminished influence of diffusion control in the uncatalyzed system relative to the catalyzed system is due to the low rate of the chemical reaction: the timescale for the chemical reaction is so large that the timescale for diffusion is comparatively small, even at high conversions and after vitrification. In contrast, diffusion control occurs well before vitrification in the catalyzed system due to the small timescale (high rate) of the chemical reaction.

The apparent activation energy of the reaction is

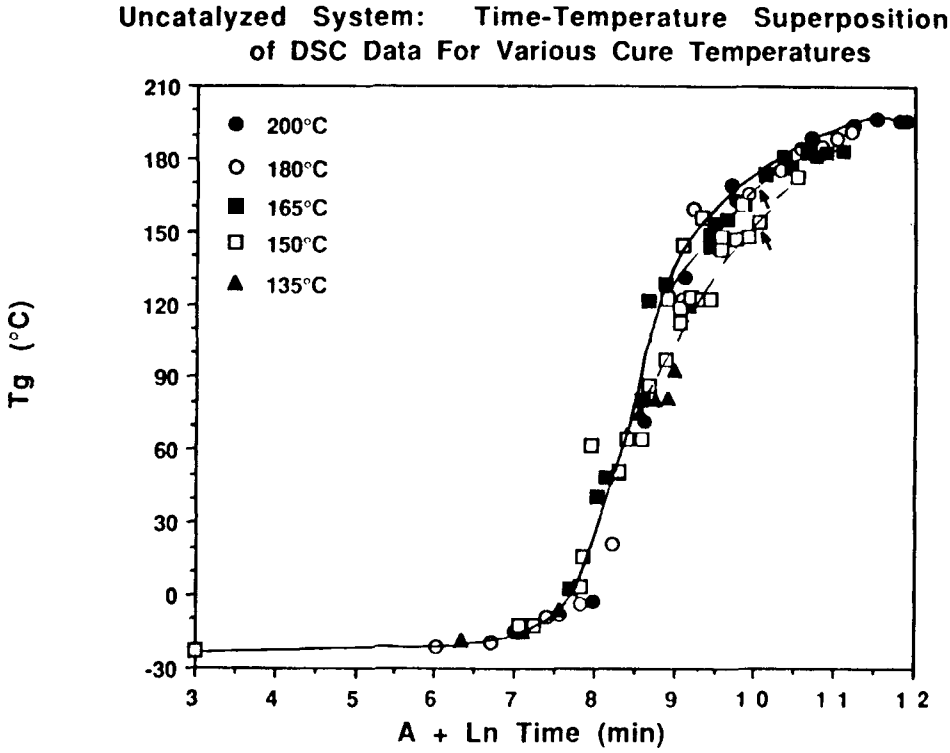


**Figure 9** Time–temperature superposition of DSC $T_g$ vs. Ln time isothermal cure data for the uncatalyzed system for cure temperatures from 135 to 200°C. Vitrification at each cure temperature is marked by arrows. Full line is hand-fit master curve; dashed lines are hand-fit deviation from master curve.

obtained by an Arrhenius plot of the shift factors used in the time–temperature superposition vs. reciprocal temperature.[6,34] No knowledge of the form of the rate expression is needed to obtain the apparent activation energy, which is assumed to be that of the overall reaction:

$$\frac{dx}{dt} = k_o e^{-E/RT_c} f(x) \tag{8}$$

where $k_o$ is the pre-exponential frequency factor for the overall reaction, $E$ is the apparent activation energy for the overall reaction, and $f(x)$ is an unknown function of $x$ and is assumed to be independent of temperature. Rearranging the equation and integrating yields:

$$\mathrm{Ln}\int_0^x \frac{dx}{f(x)} = \mathrm{Ln}k_o + \mathrm{Ln}t - \left(\frac{E}{RT_c}\right) \tag{9}$$

Since the left hand side of the equation is considered to be only a function of conversion, and because there is a one-to-one relationship between conversion and $T_g$, some function of $T_g$, $F(T_g)$, can be substituted for the left hand side of the equation:

$$F(T_g) = \mathrm{Ln}k_o + \mathrm{Ln}t - \left(\frac{E}{RT_c}\right) \tag{10}$$

To construct the kinetically-controlled master curve, $T_g$ vs. ln time curves are superposed at a low $T_g$, to insure being in the kinetically-controlled regime, with one of the curves being a reference curve at an arbitrary reference temperature (150°C in this work). The horizontal shift factor, $A(T_c)$, is the difference in ln time between two curves shifted at constant $T_g$:

$$A(T_c) = \mathrm{Ln}t_r - \mathrm{Ln}t = \frac{-E}{R}\left(\frac{1}{T_c} - \frac{1}{T_r}\right) \tag{11}$$

where the subscript $r$ pertains to the reference curve.

Figure 11 shows plots of the shift factor, $A(T_c)$, vs. $1/T_c$ for both the uncatalyzed and catalyzed systems obtained from the DSC data. The shift factors obtained by shifting isothermal conversion vs. ln time data from FTIR isothermal curing experiments

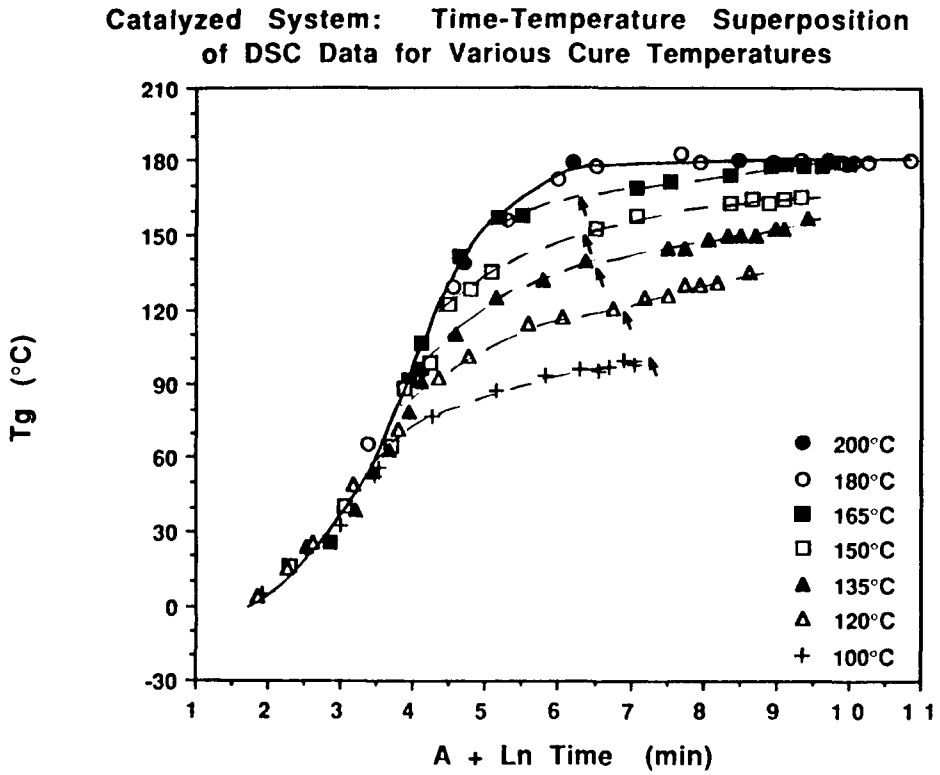


**Figure 10** Time–temperature superposition of DSC $T_g$ vs. Ln time isothermal cure data for the catalyzed system for cure temperatures from 100 to 200°C. Vitrification at each cure temperature is marked by arrows. Full line is hand-fit master curve; dashed lines are hand-fit deviation from master curve.

are also shown for the uncatalyzed system after accounting for a systematic temperature difference of 10°C between the DSC and FTIR equipment. The plots yield the apparent activation energies of 92 kJ/mol (22 kcal/mol) and 54 kJ/mol (13 kcal/mol) for the overall reactions of the uncatalyzed and catalyzed systems, respectively.

The two kinetically-controlled master curves plotted using conversion (or scaled $T_g$), rather than $T_g$ as in Figures 9 and 10, for the uncatalyzed and catalyzed systems at 150°C should superpose with a horizontal shift related to the difference in the rate constants if the expression $f(x)$ in eq. (8) is the same for both systems. However, they cannot be superposed.[8] It is observed that the master curve of the uncatalyzed system has more autocatalytic character or a lower order of reaction [i.e., $f(x) = (1 - x)^{n-1}x$ or $f(x) = (1 - x)^n$, where $n$ is the overall order of reaction and $f(x)$ is the function in eq. (8)] than that of the catalyzed system.[8,14]

Since both uncatalyzed and catalyzed systems contain active hydrogens and metal ions (phenol and metal impurities in the uncatalyzed system[1,9] and added nonylphenol/metal salt complex catalyst in the catalyzed system), it is considered that the reactions in the catalyzed system should also occur in the uncatalyzed system, but at a lower rate, due to the lower concentrations of catalytic species. Reactions, if any, which do not involve catalysts are similarly considered to occur in both systems. Consequently, the apparent activation energies of the overall reactions for the two systems are considered to be weighted averages of the various reaction steps or pathways which simultaneously occur in each system.

## FTIR Studies and Kinetic Models for the Uncatalyzed System

Isothermal FTIR curing studies were accomplished for the uncatalyzed system at cure temperatures from 190 to 220°C for times up to 1500 min ($\approx$1 day). Typical FTIR absorption spectra from 3200 to 2000 $cm^{-1}$ for one specimen, uncured and partially cured, of the uncatalyzed system are shown in Figure 12. The three peaks from 2350 to 2150 $cm^{-1}$ are as-

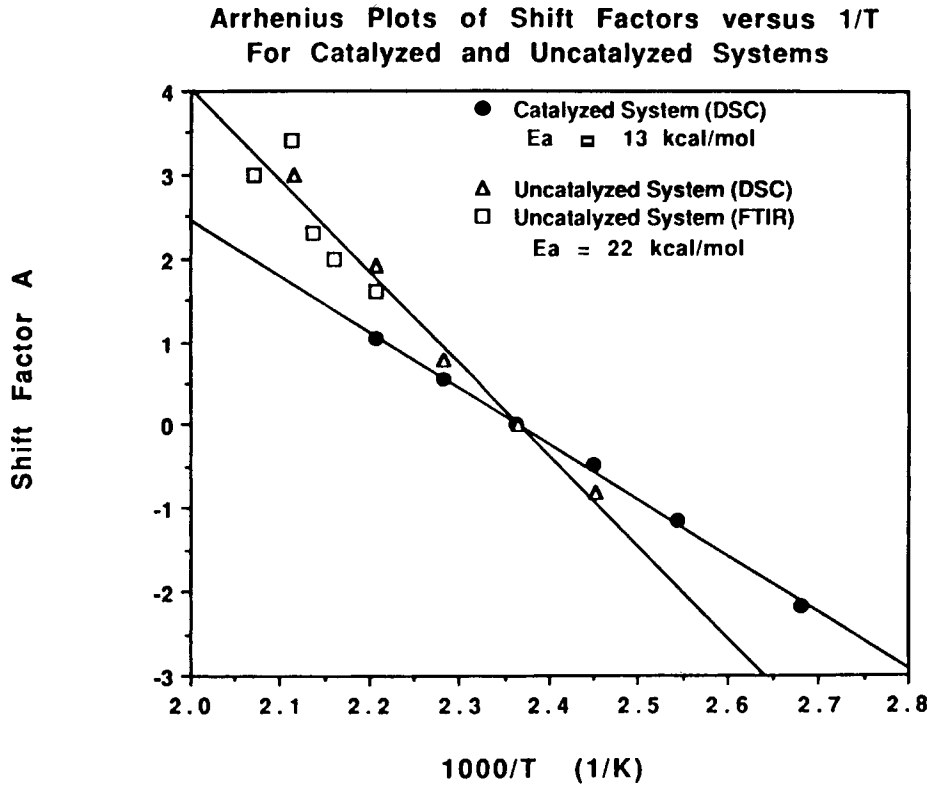


**Figure 11** Arrhenius plots of shift factors versus reciprocal temperature for catalyzed and uncatalyzed systems. The shift factors for shifting DSC $T_g$ vs. Ln time data are shown for both systems. The shift factors for shifting conversion versus Ln time FTIR data are also shown for the uncatalyzed system.

sociated with the cyanate groups, whereas the peaks from 3150 to 2800 $cm^{-1}$ are due to $CH_3$ and aromatic CH stretching. Other relevant peaks in the spectra include peaks associated with the triazine product (not shown here): the triazine peak at 1365 $cm^{-1}$ and the phenyl-oxygen-triazine stretching peak at 1565 $cm^{-1}$. During cure, the peaks associated with the cyanate decrease in intensity, whereas those associated with the triazine product increase.[2] In this work, the $CH_3$ peak height at 2970 $cm^{-1}$ is used as the internal standard.

Other researchers report that the aryl phenol precursor to the dicyanate ester monomer is present at concentrations of 0.5 to 1.5 mol % (per mole cyanate group) for conventionally synthesized and normally cleaned monomers.[9] There are no measurable peaks in the region from 3600–3400 $cm^{-1}$ (not shown), the presence of which would substantiate the presence of free or hydrogen-bonded phenol groups in the uncatalyzed system, presumably because of the low concentration of these species. There are also no measurable phenol peaks observed in the catalyzed system, which contains 1.7 mol % added nonylphenol. Consequently, the original concentration of aryl phenol in the monomer investigated may be in the range indicated by other researchers.

The peak heights of the two cyanate absorption peaks at 2270 and 2235 $cm^{-1}$ are found to be proportional during isothermal cure, with the proportionality having a slight dependence on the curing temperature, associated with an enthalpy difference of 0.3 kcal/mol.[8] Solution FTIR studies of the uncatalyzed monomer in polar solvents, dimethyl sulfoxide and methyl ethyl ketone, and a nonpolar solvent, hexane, demonstrate that the ratio of the two peaks is independent of solvent polarity.[8] Consequently, it is considered that the two cyanate peaks are not associated with "open" dimer complex and free cyanate species, as has been considered.[35] Nuclear magnetic resonance (NMR) studies of the Nuclear Overhauser Effect (NOE) for the uncatalyzed monomer at various temperatures demonstrate that no enhancement is observed for the cyanate carbon above approximately 80°C.[20]

The fractional conversion of reactant is calculated

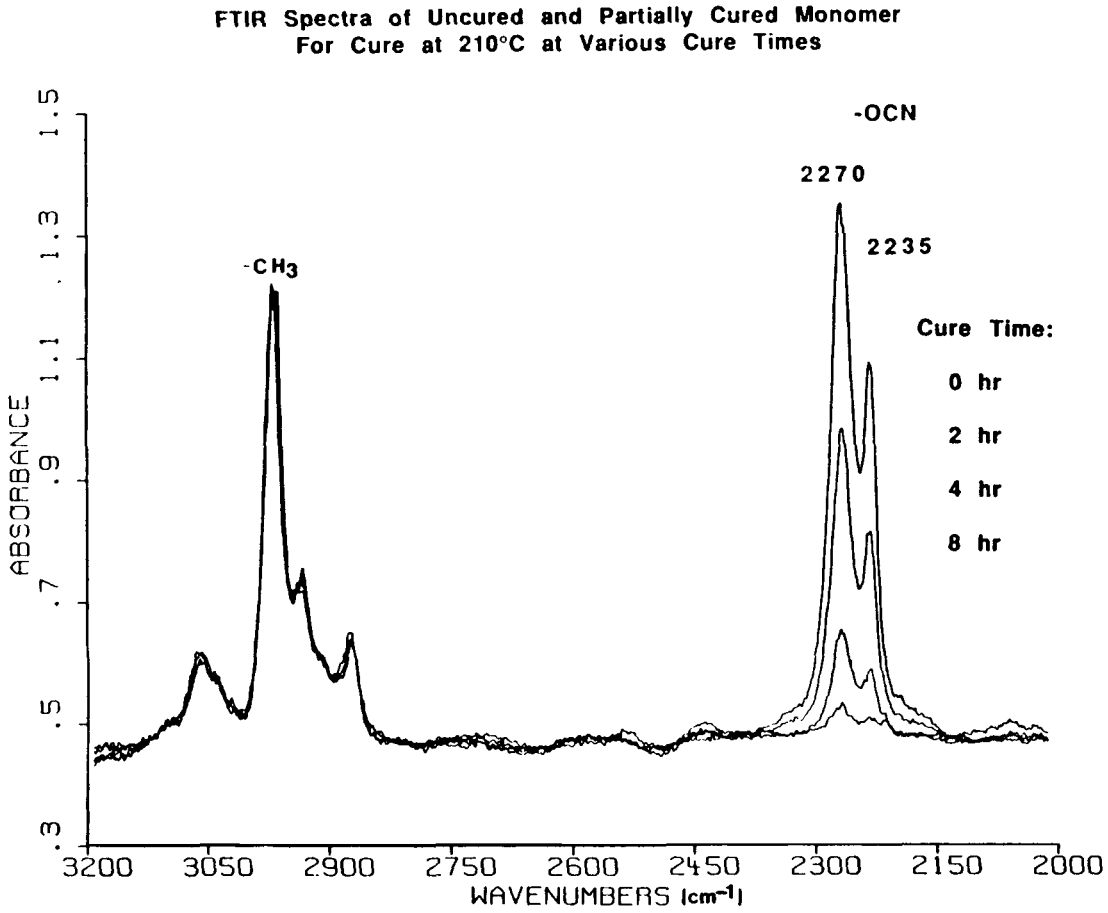


**Figure 12** FTIR spectra for the uncatalyzed system, uncured and partially cured, from 3200 to 2000 $cm^{-1}$ showing $-CH_3$ and —OCN absorption bands.

from the peak height of the cyanate peak at 2270 $cm^{-1}$, normalized by the $CH_3$ peak height:

$$x(\text{FTIR}) = \frac{(C_o - C)}{C_o} \qquad (12)$$

where $C_o$ is the normalized peak height at 2270 $cm^{-1}$ for the uncured material and C is the normalized peak height for the partially cured material. The peak at 2235 $cm^{-1}$ does not affect the peak height at 2270 $cm^{-1}$; the conversion determined from the half area of the 2270 $cm^{-1}$ peak ($\approx$2320 to 2270 $cm^{-1}$) matches that obtained by the peak height method.[8] During the initial few minutes of cure, the normalized peak height at 2270 $cm^{-1}$ remains constant, or in some cases increases, whereas the peak at 2235 $cm^{-1}$ decreases, and both triazine peaks increase. After this initial thermal "equilibration," the peak height at 2270 $cm^{-1}$ decreases and the cyanate peaks at 2270 and 2235 $cm^{-1}$ are proportional throughout isothermal cure. In the calculation of conversion from eq. (12), $C_o$ is taken as the largest initial value peak at 2270 $cm^{-1}$. The transient region, if any, is ignored in determining the kinetics of the reaction. The initial time, $t_o$, of the reaction, however, is taken as the time when the temperature first reaches the reaction temperature.

It has been asserted that the trimerization reaction will not take place if absolutely pure aromatic dicyanate esters are heated.[9] In systems without added phenol catalyst, the reaction is considered to be catalyzed by the aryl phenol impurities in conventionally synthesized dicyanate esters.[9] Although the kinetic model proposed by Bauer et al. fits their data for cure temperatures at and above 200°C to conversions of 60%, it cannot describe the present experimental findings for the uncatalyzed system at cure temperatures below 200°C, as discussed elsewhere.[8] Further, the model of Bauer et al. invokes adventitious water to start the reaction, but treats it empirically with a decaying exponential term.[9]

In order to describe the present data, an empirical

equation describes the data throughout the entire range of temperatures investigated in the FTIR and DSC work (120 to 220°C). The model can be derived from a plausible reaction scheme (see below), and is comprised of second-order and second-order autocatalytic (third-order overall) reactions:

$$\frac{dx}{dt} = k\alpha(1-x)^2 + k(1-x)^2x$$

$$= k(1-x)^2(x+\alpha) \quad (13)$$

with two adjustable parameters, the rate constant for the autocatalyzed reaction ($k$), and the ratio of the rate constants for the second-order to the second-order autocatalytic reactions ($\alpha$), both of which are assumed to vary with temperature. Other kinetic models were tested, but were not found to describe the data throughout the entire range of cure temperatures investigated, even though some had more adjustable parameters than the model proposed in this work.[8] The model is similar in form to those derived independently by other researchers for the reaction of bisphenol A dicyanate; their model of the uncatalyzed reaction is comprised of first order and first-order autocatalytic reactions, whereas their model of the catalyzed reaction is second-order.[12,13] Another group of researchers has also concluded that the reaction of bisphenol A dicyanate was autocatalytic for the uncatalyzed system and second-order for the catalyzed system.[29]

Possible reactions of dicyanate esters are shown in Figure 13. In contrast to the models proposed by Bauer et al.[9] and by Bonetskaya et al.,[10] it is considered in this work that the reaction of cyanate ester with aryl phenol is an equilibrium reaction, as has been proposed by some other researchers.[2,36] The equilibrium reaction shifts toward the imidocarbonate intermediate with increasing basicity (triazine concentration) and decreasing temperature. The imidocarbonate intermediate reacts stepwise with two cyanate esters to form the triazine ring and to regenerate the aryl phenol. When metal complexing ions are present, as added catalyst in the catalyzed system or impurities in the uncatalyzed system, the imidocarbonate and dimer intermediates are assumed to be stabilized by the metal complex.

The principal reaction of adventitious water with cyanate ester yields an intermediate, which is stabilized by carbamate formation, although the intermediate can also react to yield triazine.[36] The degree of carbamate formation has been found to be affected by the type of metal catalyst used, with zinc octoate catalyst promoting more carbamate formation than copper or cobalt carboxylates.[37] Although the reactions of cyanate ester with adventitious water can easily be included in the mechanism, their addition increases the number of equations from one to two simultaneous differential equations, as well as increasing the number of adjustable parameters from two to five (four rate constants plus the concentration of adventitious water).[8] Consequently, the reactions with adventitious water are ignored in the following derivation in order to obtain the simpler empirical equation with two adjustable parameters, which is found to fit the data.

The equilibrium constants for the reactions to form the imidocarbonate and metal ion-complexed imidocarbonate are defined as:

$$K_1 = \frac{k_1}{k_1'} = \frac{I}{CHT}$$

$$K_1^* = \frac{k_1^*}{k_1'^*} = \frac{I^*}{CHM} \quad (14)$$

where $I$, $I^*$, $C$, $H$, $T$, and $M$ are the concentrations of imidocarbonate, metal ion-complexed imidocarbonate, cyanate ester, active hydrogen compounds (aryl phenol and nonylphenol), triazine, and metal ions, respectively. The superscript * refers to reactions catalyzed by metal ions rather than triazine. The concentrations of the imidocarbonate intermediate and active hydrogen compounds are related by mass balance:

$$H_o = H + I + I^* \quad (15)$$

where $H_o$ is the initial concentration of active hydrogen (i.e., aryl phenol impurity plus added nonylphenol catalyst, the latter being zero in the uncatalyzed system). Consequently, the concentration of active hydrogen compounds can be found by combining the above equations:

$$H = \frac{H_o}{1 + K_1CT + K_1^*CM} \quad (16)$$

Assuming that the reactions of cyanate ester with imidocarbonate and metal-complexed imidocarbonate (steps 2 and 2*) are slow, relative to the addition of the second cyanate ester to the dimer complex (steps 3 and 3*), the disappearance of cyanate ester can be written as:

$$-\frac{dC}{dt} = \frac{2k_2K_1H_oC^2T + 2k_2^*K_1^*H_oMC^2}{1 + K_1CT + K_1^*CM} \quad (17)$$

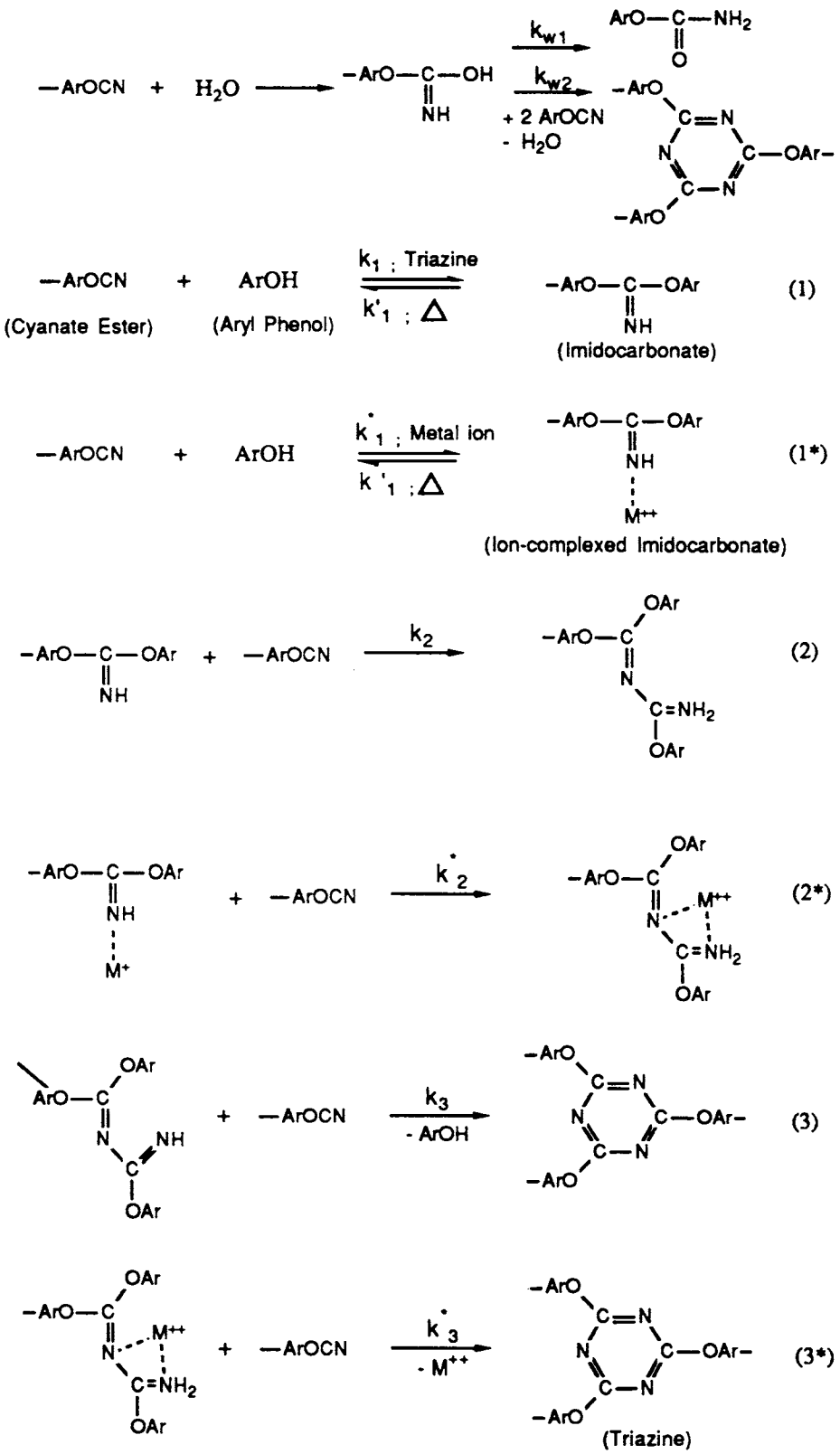


**Figure 13** Proposed relevant reactions of dicyanate ester/polycyanurate system.

Assuming that $1 \gg K_1CT + K_1^*CM$, that is, that the equilibrium steps (1 and 1*) are shifted to the left, as would be expected for low conversions (small $T$) and/or high temperatures and for relatively low concentrations of metal, then

$$-\frac{dC}{dt} = 2k_2K_1H_oC^2T + 2k_2^*K_1^*H_oMC^2 \quad (18)$$

In terms of conversion of cyanate ester:

$$\frac{dx}{dt} = \frac{2}{3}k_2K_1H_oC_o^2(1-x)^2x + 2k_2^*K_1^*H_oC_o^2M(1-x)^2 \quad (19)$$

where $C_o$ is the initial concentration of cyanate ester.

Thus, the two constants in the empirical rate eq. (13), $k$ and $\alpha$, are related to the kinetic mechanism:

$$k = \tfrac{2}{3}k_2K_1H_oC_o^2 \text{ and } \alpha = \frac{3k_2^*K_1^*M}{k_2K_1}.$$

It is preferable to obtain the model parameters $k$ and $\alpha$ by the differential method. However, due to the scatter in the data, the integral method is used. To obtain the best values of $k$ and $\alpha$ for isothermal FTIR studies, the rate eq. (13) is numerically integrated using various values of $k$ and $\alpha$. The best values are obtained by a least square fit, minimizing $\text{Chi}^2$:

$$\text{Chi}^2 = \sum_1^i [x(t) - x(t)_{\text{calculated}}]^2 \quad (20)$$

where $i$ is the number of data points taken logarithmically during an isothermal curing experiment (generally $i = 88$), $x(t)$ is the experimental value of conversion at time $t$, and $x(t)_{\text{calculated}}$ is the calculated value.

The activation energies for the reactions are obtained from the Arrhenius plots shown in Figure 14, assuming that the rate constants $k$ and $\alpha k$ of eq. (13) follow the Arrhenius form. The composite activation energy for the autocatalyzed reaction rate constant $k$ is found to be 120 kJ/mol (29 kcal/mol), whereas the composite activation energy for the second-order reaction rate constant $\alpha k$ is 44 kJ/mol (11 kcal/mol). The relatively large scatter in the data for the second order rate constant $\alpha k$ is presumed to be due to the effects of adventitious water.

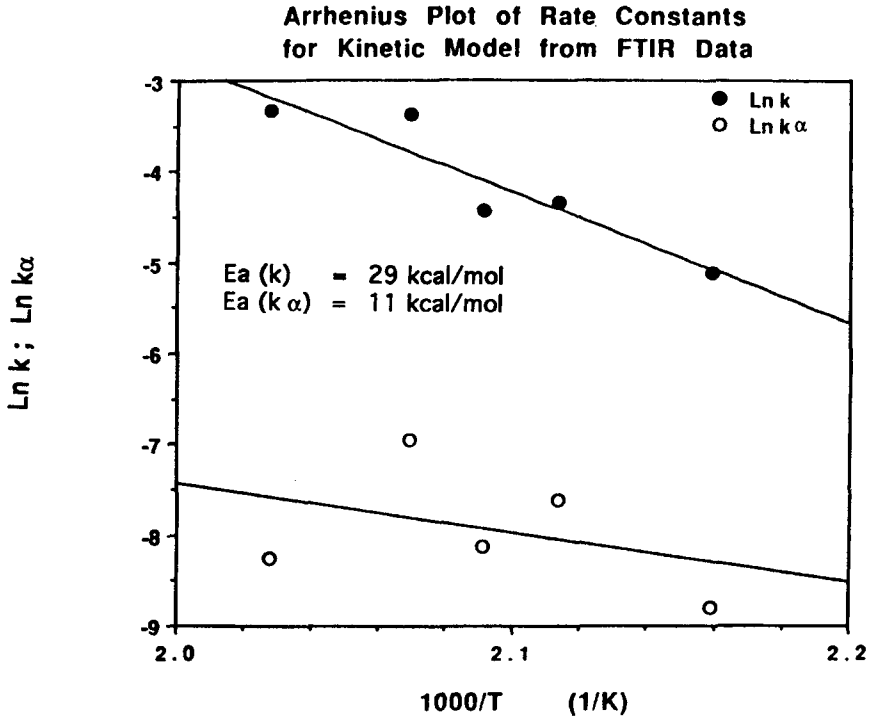


**Figure 14** Arrhenius plot of the Ln of the rate constants for the second-order autocatalytic and second-order reactions, $k$ and $\alpha k$, respectively, vs. reciprocal temperature, from FTIR isothermal studies of the uncatalyzed system. The composite activation energies are found to be 29 and 11 kcal/mol, respectively.

The magnitude and relative temperature dependence of the two rate constants, $k$ and $\alpha k$, are consistent with the proposed model, with the initial concentration of active hydrogen compounds, $H_o$, being incorporated in both rate constants, and the concentration of metal ions, $M$, being incorporated only in the rate constant for the second-order reaction, $\alpha k$. The absolute value of the rate constants are $k = 0.012$ and $k\alpha = 0.00032$ min$^{-1}$ for the second-order autocatalyzed and second-order reactions at 200°C, respectively. The values of both terms are small due to the incorporation of the trace aryl phenol impurity concentration, with the value of the pre-exponential frequency factor for the second-order reaction being much lower than that of the second-order autocatalyzed reaction, because the small concentration of metal ion impurities is also incorporated into the former term. The temperature dependence of the two constants is also consistent with the model, with the second-order reaction having a lower activation energy since it is facilitated by metal ions. (Note that the results could be interpreted differently with the second order reaction being facilitated by water rather than metal ion impurities.)

## Application of Kinetic Model to DSC Data for Uncatalyzed System

The proposed mathematical model with parameters determined from FTIR studies over a limited temperature range (190 to 220°C), is tested by its application to the DSC data over a wider range of temperatures (120 to 200°C). The kinetic rate expression [eq. (13)] is numerically integrated to determine the times to reach specific conversions for each DSC cure temperature. The conversion data are then transformed to $T_g$, using the modified DiBenedetto relationship [eq. (2)]. $T_g$ vs. time curves, rather than conversion vs. time curves, are used for comparison because $T_g$ is more sensitive than conversion at high conversions due to the curvature of the $T_g$ vs. conversion relationship, and because $T_g$ is more accurately measured.[6] The calculated $T_g$ vs. ln time curves are shown as the solid

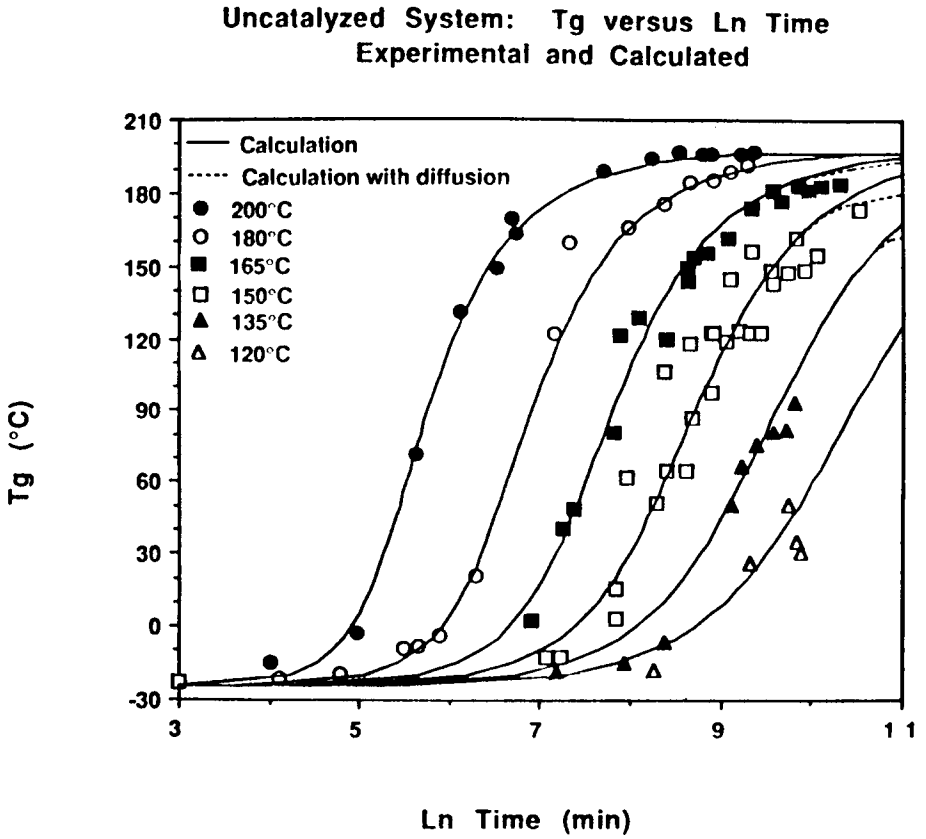


**Figure 15** Calculated vs. experimental DSC $T_g$ vs. Ln time curves for cure temperatures from 120 to 200°C for the uncatalyzed system. Parameters determined from FTIR studies were used in the calculations.

lines in Figure 15, with the symbols representing the experimental DSC data. The pre-exponential frequency factors and activation energies determined from the FTIR work were used in the calculations, after accounting for a systematic temperature difference of 10°C between the FTIR and DSC (with DSC temperatures being 10°C higher); no other fitting of the DSC data was made. The agreement between the experimental and calculated data is satisfactory for all cure temperatures studied throughout the entire range of cure. The fact that the proposed mechanism, which was determined from experimental FTIR studies at cure temperature from 190 to 220°C, fits the DSC experimental data for cure temperatures as low as 120°C, demonstrates that the model is a useful mathematical description of the reaction.

Diffusion control was not incorporated into the model of the uncatalyzed reaction because the rate of reaction in the absence of diffusion control is relatively slow with respect to the rate of diffusion. In order to test this supposition, diffusion is incorporated into the uncatalyzed model using the same diffusion parameters as were found for the catalyzed system (see below), since the diffusion rates in the two systems should be similar. The dashed lines in Figure 15 show that the effect of diffusion in the uncatalyzed system is not significant except at the longest times investigated and after vitrification.

## Application of Kinetic Model to DSC Data for Catalyzed System

The catalysts in the catalyzed system are nonylphenol and copper naphthenate. The nonylphenol is assumed to catalyze the reaction by the formation of imidocarbonate intermediates,[2,9] as presumably did the aryl phenol impurity in the uncatalyzed system. The metal salt complex is assumed to facilitate the reaction by complexing with the intermediates.[2,10] Both metallic[2] and aryl phenol impurities[9] are known to be present in the uncatalyzed system. Consequently, it is assumed that the reactions in the catalyzed and uncatalyzed systems are the same and that the model used to describe the uncatalyzed system (which neglects adventitious water) should be applicable to the catalyzed system, without a change in the activation energies of the second-order autocatalyzed and second-order reactions. The pre-exponential frequency factors for the reactions should be increased, however, due to the increased concentration of catalysts. Since the exact concentrations of the impurities in the uncatalyzed system are not known, the two pre-exponential frequency factors for the catalyzed system will be treated as adjustable parameters to fit the data.

In the reaction model for the catalyzed system, diffusion control must be taken into account due to the relatively high rate of the chemical reaction. Due to decreasing molecular mobility as the material cures, the values of the observed rate constants decrease in the diffusion-controlled regime. It is assumed that the timescale of the reaction, the reciprocal of the observed rate constant, is equal to the timescale of diffusion plus the timescale of the chemical reaction in the absence of diffusion:

$$\frac{1}{k_i} = \frac{1}{k_{i,c}} + \frac{1}{k_d} \tag{21}$$

where $k_i$ is the observed rate constant, $i = 1$ for the autocatalyzed reaction and 2 for the second-order reaction, $k_{i,c}$ is the Arrhenius rate constant for the kinetically-controlled reaction, and $k_d$ is the reciprocal timescale of diffusion. The timescale of diffusion is the distance species need to diffuse divided by the rate of diffusion. The timescale of diffusion will increase with increasing conversion due to increasing distance between diffusing species and due to the decreasing rate of diffusion caused by decreasing molecular mobility. In this work, the effect of conversion on the diffusion lengthscale is not explicitly considered. The timescale of diffusion is considered to be dependent only on free volume and temperature. The Doolittle free volume equation, modified by the inclusion of temperature dependence as in the Macedo and Litovitz equation, is applied[38]:

$$k_d = A \exp\left(-\frac{E_d}{RT_c}\right)\exp\left(-\frac{b}{f}\right) \tag{22}$$

where $A$ and $b$ are considered to be adjustable parameters and $E_d$ is the activation energy of the diffusion process. The free volume $f$ is the equilibrium free volume given by the interval from $T_g$, using the universal constants obtained from the Williams–Landel–Ferry (WLF) equation[39]:

$$f = 0.00048\,(T_c - T_g) + 0.025 \tag{23}$$

where $T_c$ is the cure temperature. Use of the above equilibrium equation incorrectly underestimates the total non-equilibrium free volume, and predicts that the free volume in the non-equilibrium glassy polymer should be zero at Kauzmann's temperature, 52°C below $T_g$. Further, the kinetics of the decreasing free volume due to physical aging in the glass transition and glassy states are neglected in the

model. However, since the reaction does not enter the glassy state for the timescales studied, but remains in the rubbery or glass transition regions, the equilibrium equation is used as a first approximation. In our laboratory, a similar approach was used to describe the diffusion-controlled regime in a high-$T_g$ epoxy/amine system, but the temperature-activated term was not needed to describe those data.[6-8] Other researchers have successfully used the diffusion model with an activation energy to describe the diffusion controlled reaction kinetics in a different high-$T_g$ aromatic epoxy/amine system.[40] For the catalyzed dicyanate ester/polycyanurate system, the parameters $k_{do}[=A \exp(-E_d/RT)]$ and $b$ are found to be approximately 100 and 0.25 at 150°C, respectively, from plots of ln $k_d$ [from eq. (22)] vs. $1/f$ [from eq. (23)].[8] The value of $b$, being less than the ideal value of 1 in the Doolittle equation, reflects that the free volume for the dicyanate ester system is greater than that predicted by the universal WLF relationship. A value of $b$ of 0.2 was found for the epoxy/amine system studied in this laboratory,[7,8] whereas a value of 1.1 was found by the researchers investigating another epoxy/amine system.[40] The activation energy for diffusion is found to be 140 kJ/mol (33 kcal/mol) by a plot of ln $k_{do}$ vs. $1/T$.[8] This activation energy is in the range of that for the glass transition (i.e., backbone motion) and also agrees with the results of the other researchers, who found that the activation energy for diffusion in their high-$T_g$ epoxy/amine system was 143 kJ/mol (34.2 kcal/mol).[40] The value of $A$, determined after the value of $E_d$ had been obtained, is $1 \times 10^{19}$ min$^{-1}$.

The calculated and experimental $T_g$ vs. ln time data for the catalyzed system are shown in Figure 16. The experimental data are found to be satisfactorily described by the model with rate constants of 0.017 and 0.050 min$^{-1}$ for the second-order autocatalyzed and second-order reactions at 150°C, respectively, using the activation energies that describe the uncatalyzed system.

Assuming that the proposed model is correct and that the concentration of active hydrogen compound is incorporated into both rate constants, whereas the metal ion is incorporated only into the second-order reaction, the original aryl phenol and equiv-

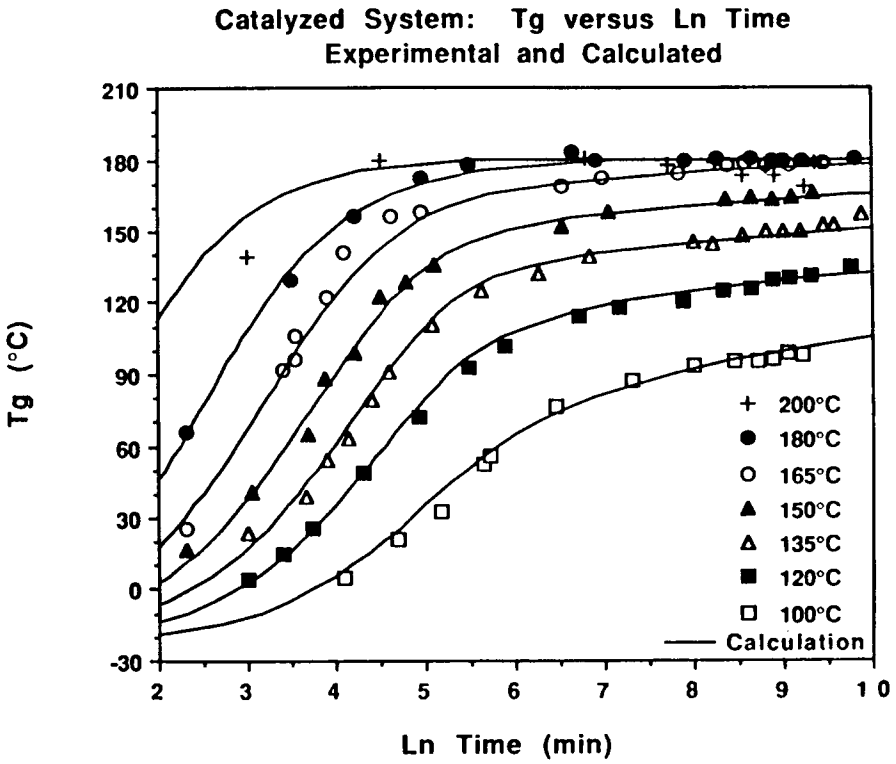


**Figure 16** Calculated vs. experimental DSC $T_g$ vs. Ln time curves for cure temperatures from 100 to 200°C for the catalyzed system. The kinetic model is that used for the uncatalyzed system with a change in the pre-exponential frequency factors and including diffusion control.

alent metal ion concentrations can then be estimated from the increase in the rate constants due to the added catalyst (using the rate constants for the uncatalyzed system of 0.00037 and 0.00013 $min^{-1}$ at 150°C for the DSC data). The addition of the nonylphenol catalyst is then assumed to increase both pre-exponential frequency factors by 46 times, which corresponds to a concentration of aryl phenol impurity of 0.1 mol % in the monomer, whereas the addition of metal is assumed to increase the pre-exponential frequency factor of the second-order reaction by 8.3 times, corresponding to an equivalent metallic ion concentration of approximately 20 ppm. In comparison, Bauer et al. predict 0.5 to 1.5 mol % for aryl phenol impurities,[9] whereas the concentration of metal ions in commercial dicyanate ester resin is less than 10 ppm.[2] The relative amounts of phenol and metal catalysts could be varied in further research to verify their respective roles in the reaction. It is also noted that different metals and complexing agents will affect the activity of the metal.[11] The effects of adventitious water, neglected in the present model, should also be investigated.

## Application of Cure Kinetics to TBA Studies: Experimental and Calculated TTT Diagrams

From isothermal TBA cure studies of the uncatalyzed and catalyzed systems, the times to macroscopic gelation and vitrification are determined from the maxima in the logarithmic decrement curves. These experimental times are plotted vs. cure temperature to construct time–temperature–transformation (TTT) isothermal cure diagrams[3,4] for the uncatalyzed and catalyzed systems, as shown in Figures 17 and 18.

From the apparent activation energy of the reaction and from the kinetically-controlled DSC master curve of $T_g$ vs. ln time data, iso-$T_g$, gelation, and vitrification contours can be calculated in the kinetically-controlled reaction regime from eq. (11).[6,27,34] However, for the catalyzed system, vitrification occurs after the onset of diffusion control and cannot be calculated by this procedure. A further complication arises for both systems since the kinetic model is comprised of two competing parallel reactions with different activation energies. Con-

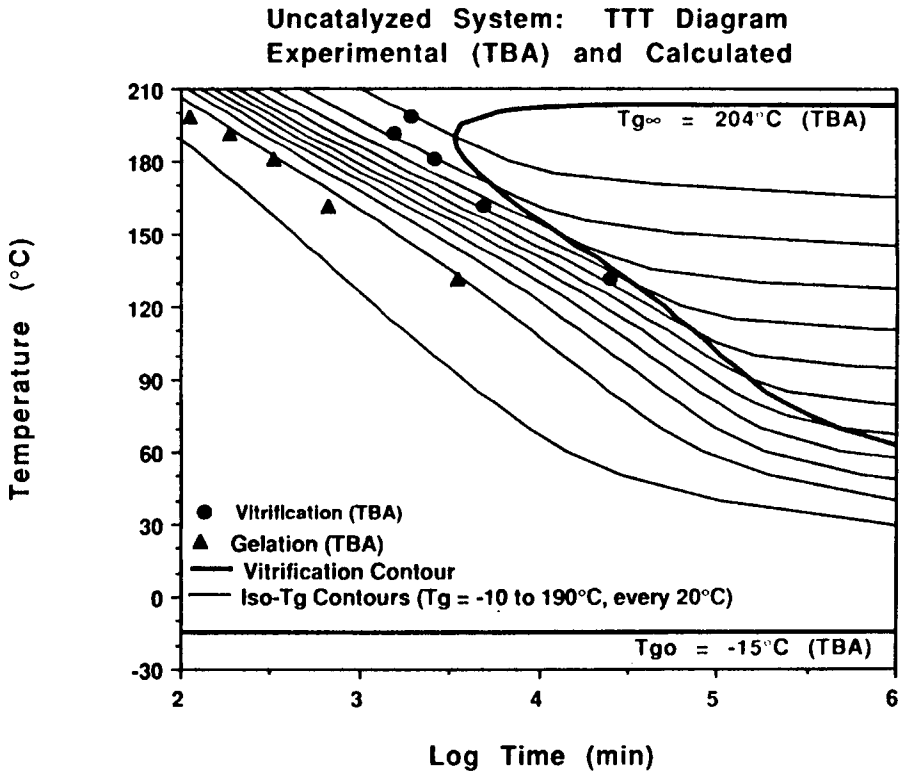


**Figure 17** TTT isothermal cure diagram for the uncatalyzed system, showing experimental TBA gelation and vitrification contours, as well as calculated contours based on the kinetic model of the reaction.

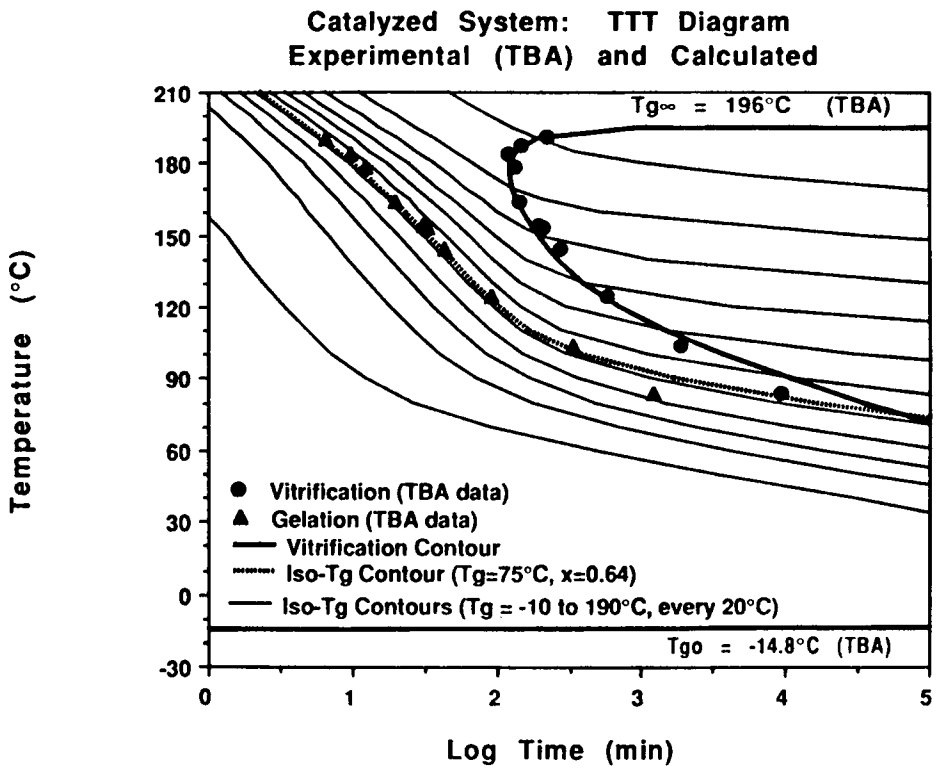


**Figure 18** TTT isothermal cure diagram for the catalyzed system, showing experimental TBA gelation and vitrification contours, as well as calculated contours based on the kinetic model of the reaction.

sequently, although the apparent kinetically-controlled master curve for each system is applicable (within the scatter of the data) for the cure temperatures and times investigated, they cannot be extrapolated. In fact, with two competing parallel reactions with different activation energies, no master curve is obtained when shifting calculated $T_g$ vs. ln time curves for various cure temperatures based on the proposed kinetic model.

The TTT isothermal cure diagrams for the systems studied are therefore calculated from the proposed kinetic model with diffusion control incorporated, which was developed from FTIR isothermal cure studies on the uncatalyzed system and was successfully extrapolated to describe the DSC isothermal cure studies of both systems. The calculation is compared to the experimental data and provides an additional check on the applicability of the model. The vitrification curve, the locus of cure times at which $T_g = T_c$, is calculated and compared to the experimental vitrification data. Ideal molecular gelation should theoretically occur at a conversion of 50%.[5] Thus, the ideal molecular gelation contour is an iso-$T_g$ contour for $x = 0.5$ (not shown). Iso-$T_g$ contours are also calculated from the kinetic model.

The experimental and calculated gelation and vitrification contours on the TTT diagram for the uncatalyzed system do not agree, as is apparent in Figure 17. The experimental TBA data result from a faster rate of reaction than is observed in the DSC data, from which the theoretical contours were calculated. Since the FTIR studies agreed with the DSC studies, it is considered that the faster rate of reaction observed in TBA studies for the uncatalyzed system results from interaction of the fiberglass braid substrate with the monomer; in particular, hydroxyl groups on the surface of the heat-cleaned fibers are assumed to catalyze the reaction. Such groups would not alter the rate of the catalyzed reaction if the concentration of catalyst in the monomer is much greater than that on the surface of the fibers.

Figure 18 shows the experimental and calculated TTT diagram for the catalyzed system. The experimental and calculated vitrification contours are in agreement, presumably since the catalytic effect of the fiberglass braid is overwhelmed by the effects of the added catalysts. Macroscopic gelation is found to be an iso-conversion (iso-$T_g$) event for cure temperatures above 100°C, but not at a conversion of 0.50, as would be expected for idealized molecular gelation, but rather at a $T_g$ of approximately 75°C

and a conversion of 0.64. Other work from this laboratory revealed that macroscopic gelation of the uncatalyzed system occurred at a conversion of 0.65 ± 0.02 from a change in slope of isothermal modulus vs conversion data.[18] Other researchers have similarly found that the gel point, as measured by solubility in various solvents, occurs in the vicinity of 0.58 to 0.65.[1,22,24,29] One explanation for the delay in gelation from the ideal value of 0.50 is the presence of non-ideal intramolecular reactions prior to gelation. Another explanation, postulated by one group of researchers, is that the reaction is heterogeneous (i.e., the reaction is localized) and, thus, the distribution of molecular weight would deviate from that predicted by Flory's theory.[29] However, another group of researchers found that gelation does occur at the ideal value of 0.50, and implicitly suggests that the shift in the conversion at gelation is due to monofunctional impurities in the monomers used by other researchers.[41]

## CONCLUSIONS

The cure of a dicyanate ester/polycyanurate system, both uncatalyzed and catalyzed, has been studied. The same one-to-one relationship between dimensionless $T_g$ and conversion is found for both systems. Time–temperature superposition of $T_g$ vs. ln time data to form kinetically-controlled master curves for both systems suggests that diffusion control is only significant in the catalyzed system, where the timescale of chemical reaction in the absence of diffusion is low. The apparent activation energies of the overall reactions for the uncatalyzed and catalyzed systems are found to be 92 kJ/mol (22 kcal/mol) and 54 kJ/mol (13 kcal/mol). A kinetic model of the uncatalyzed system is determined from *in-situ* FTIR cure studies at five temperatures from 190 to 220°C. The empirical model is comprised of two parallel competing reactions, both second order with respect to dicyanate, one of which is autocatalyzed. Experimental curves are fit by the rate expression throughout the entire range of cure. The composite activation energies for the two reactions are found to be 120 and 44 kJ/mol (29 and 11 kcal/mol), respectively. The proposed model is tested by its application to the DSC and TBA data. Calculated $T_g$ vs. ln time curves fit the DSC experimental data for the uncatalyzed system at the cure temperatures studied (120 to 200°C) throughout the entire range of cure. Calculations were based on the proposed mathematical model of the reaction, and the rate constants and activation energies used were those obtained from the FTIR studies. The model with the same activation energies, and with diffusion control incorporated, also satisfactorily describes the DSC $T_g$ vs. ln time data for the catalyzed system. Iso-$T_g$ and vitrification contours on the time–temperature–transformation (TTT) isothermal cure diagram are calculated for each system from the kinetic model. It is found that macroscopic gelation obtained from TBA data on the catalyzed system falls on an iso-$T_g$ contour corresponding to a conversion of 0.64 for cure temperatures from 100 to 200°C. In summary, the proposed mathematical description of the dicyanate ester/polycyanurate curing reactions, with diffusion control incorporated, satisfactorily describes the experimental data for both uncatalyzed and catalyzed systems over a wide temperature range and throughout the curing process, and is a useful model of the reaction.

The authors gratefully acknowledge the interest of David A. Shimp, the work of Wallace M. Craig, Jr. in the synthesis of the monomer, and the financial support of Rhône–Poulenc High Performance Resins.

## NOMENCLATURE (PARTIAL LISTING)

| | |
|---|---|
| $A$ | Parameter in Doolittle free-volume equation |
| $A(T_c)$ | Shift factor between two $T_g$ vs. ln time curves at different cure temperatures |
| $b$ | Parameter in Doolittle free-volume equation |
| $C$ | Concentration of cyanate groups |
| $C_o$ | Initial concentration of cyanate groups |
| $E$ | Apparent activation energy for overall reaction |
| $E_d$ | Activation energy for diffusion of reacting species |
| $f$ | Free volume fraction |
| $H$ | Concentration of active hydrogen compounds |
| $H_o$ | Initial concentration of active hydrogen compounds |
| $I$ | Concentration of imidocarbonate |
| $I^*$ | Concentration of metal ion-complexed imidocarbonate |
| $k$ | Parmaeter in $T_g$ vs. conversion equation incorporating effect of dangling chains on $T_g$; Also: Rate constant for second-order autocatalyzed reaction in dicyanate ester/polycyanurate system |
| $k_o$ | Pre-exponential frequency factor for the overall reaction |
| $K$ | Parameter in eq. (3), incorporating effect of crosslinks on $T_g$ |
| $M$ | Concentration of metal ions |
| $P(F_C^{in})$ | Probability of finding a finite, rather than infinite, chain looking onto a cyanate group |
| $P(F_C^{out})$ | Probability of finding a finite, rather than |

| | |
|---|---|
| | infinite, chain looking out from a cyanate group |
| $R$ | Gas constant |
| $t$ | Isothermal cure time |
| $t_r$ | Reference isothermal cure time |
| $T$ | Concentration of triazine |
| $T_c$ | Isothermal cure temperature |
| $T_g$ | Glass transition temperature |
| $T_{g\infty}$ | Glass transition temperature of fully cured material |
| $T_{g\infty}$ | Glass transition temperature of fully cured material |
| $T_r$ | Reference isothermal cure temperature |
| $x$ | Fractional conversion of cyanate in the dicyanate ester/polycyanurate system |
| $X$ | Crosslink density |
| $\alpha$ | Ratio of rate constants for second-order autocatalytic and second-order reactions |
| $\Delta H_r$ | Residual heat of DSC exotherm |
| $\Delta H_T$ | Total heat of DSC exotherm for uncured material |
| $\lambda$ | Parameter in DiBenedetto equation relating $T_g$ to conversion |
| $\Psi$ | Parameter in $T_g$ vs. conversion relation incorporating effect of non-Gaussian nature of crosslinks at high crosslink density on $T_g$ |

## REFERENCES


1. D. A. Shimp, S. J. Ising, and J. R. Christenson, *International SAMPE Symposium and Exhibition Proceedings,* Reno, NV, **35**(1), 1045–1056 (1990).
2. D. A. Shimp, S. J. Ising, and J. R. Christenson, *International SAMPE Symposium and Exhibition Proceedings,* Reno, NV, **34**(1), 222–233 (1989).
3. J. K. Gillham, *Polym. Eng. Sci.,* **26**(20), 1429 (1986).
4. J. B. Enns and J. K. Gillham, *J. Appl. Polym. Sci.,* **28,** 2567 (1983).
5. K. Fukui and T. Yamabe, *J. Polym. Sci.,* **45,** 305 (1960).
6. G. Wisanrakkit and J. K. Gillham, *J. Coating Tech.,* **62**(783), 35 (1990); *J. Appl. Polym. Sci.,* **41,** 2885 (1990).
7. S. L. Simon and J. K. Gillham, *J. Appl. Polym. Sci.,* **46,** 1245 (1992).
8. S. L. Simon, Ph.D. Thesis, Department of Chemical Engineering, Princeton University, January 1992.
9. M. Bauer, J. Bauer, and G. Kuhn, *Acta Polymerica,* **37**(11/12), 715 (1986).
10. A. K. Bonetskaya, V. V. Ivanov, M. A. Kravchenko, V. A. Pankratov, Ts. M. Frenkel, V. V. Korshak, and S. V. Vinogradova, *Vysokomol. Soved.,* **A22**(4), 766 (1980).
11. A. Osei-Owusu, G. C. Martin, and J. T. Grotto, *Polym. Eng. Sci.,* **31**(22), 1604 (1991).
12. A. Osei-Owusu and G. C. Martin, *Polym. Eng. Sci.,* **32,** 535 (1992).
13. A. Osei-Owusu and G. C. Martin, *ACS Polym. Mat. Sci. Eng. Prprt.,* **65,** 304 (1991).
14. S. L. Simon, J. K. Gillham, and D. A. Shimp, *ACS Polym. Mat. Sci. Eng. Prprt.,* **62,** 96 (1990).
15. S. L. Simon and J. K. Gillham, *ACS Polym. Mat. Sci. Eng. Prprt.,* **63,** 760 (1990).
16. S. L. Simon and J. K. Gillham, *ACS Polym. Mat. Sci. Eng. Prprt.,* **66,** 453 (1992).
17. S. L. Simon, *ACS Div. of Polym. Chem. Polym. Prpr.,* **32**(2), 182–184 (1991).
18. S. L. Simon and J. K. Gillham, *ACS Polym. Mat. Sci. Eng. Prprt.,* **66,** 277 (1992).
19. S. L. Simon and J. K. Gillham, *ACS Polym. Mat. Sci. Eng. Prprt.,* **66,** 502 (1992).
20. T. Fang, Private Communication, AT&T Bell Labs (1991).
21. T. Fang, *Macromolecules,* **23,** 4553 (1990).
22. J. P. Armistead and A. W. Snow, *ACS Polym. Mat. Sci. Eng. Prprt.,* **66,** 457 (1992).
23. J. M. Barton, D. C. L. Greenfield, I. Hamerton, and J. R. Jones, *Polym. Bull.,* **25,** 475 (1991).
24. A. M. Gupta and C. W. Macosko, *Makromol. Chem. Macromol. Symp.,* **45,** 105 (1991).
25. J. K. Gillham, in *Developments in Polymer Characterisation,* J. V. Dawkins, Ed., Applied Science, London, 1982, pp. 157–227.
26. V. Micro, Z. Q. Cao, F. Mechin, J. P. Pascault, *ACS Polym. Mat. Sci. Eng. Prprt.,* **66,** 451 (1992).
27. P. Pang and J. K. Gillham, *J. Appl. Polym. Sci.,* **37,** 1969 (1989).
28. X. Wang and J. K. Gillham, *J. Appl. Polym. Sci.,* **45,** 2127 (1992).
29. A. M. Gupta and C. W. Macosko, *ACS Polym. Mat. Sci. Eng. Prprt.,* **66,** 447 (1992).
30. L. E. Nielsen, *J. Macromol. Sci. Rev. Macromol. Chem.,* **C3,** 69 (1969).
31. J. P. Pascault and R. J. J. Williams, *J. Polym. Sci. Part B Polym. Phys.,* **28,** 85 (1990).
32. A. Hale, C. W. Mocosko, and H. E. Bair, *Macromolecules,* **24**(9), 2610 (1991).
33. D. R. Miller and C. W. Macosko, *Macromolecules,* **9**(2), 206 (1976).
34. S. Gan, J. K. Gillham, and R. B. Prime, *J. Appl. Polym. Sci.,* **37,** 803 (1989).
35. J. L. Cercena, Ph. D. Thesis, Department of Chemistry, University of Connecticut, 1984.
36. E. Grigat and R. Putter, *Angew. Chem. Internat.,* **6**(3), 206 (1967).
37. D. A. Shimp and S. J. Ising, *ACS Polym. Mat. Sci. Eng. Prprt.,* **66** (1992).
38. P. B. Macedo and T. A. Litovitz, *J. Chem. Phys.,* **42,** 245 (1969).
39. M. L. Williams, R. F. Landel, and J. D. Ferry, *J. Am. Chem. Soc.,* **77,** 3701 (1955).
40. W. M. Sanford and R. L. McCullough, *J. Polym. Sci. Part B Polym. Phys.,* **28,** 973 (1990).
41. M. Bauer, J. Bauer, and S. Jahrig, *ACS Polym. Mat. Sci. Eng. Prprt.,* **66,** 455 (1992).


*Received November 19, 1990*
*Accepted March 11, 1992*